UNIVERSITÀ DEGLI STUDI DI PADOVA

Dipartimento di Fisica e Astronomia "Galileo Galilei"

Master Degree in Physics

Final Dissertation

Electronic properties of twisted bilayer graphene

Thesis supervisor

Prof./Dr. Luca Dell'Anna

Thesis co-supervisor

Prof./Dr. Francesco Ancilotto

Candidate

Giuseppe Meneghini

Academic Year 2019/2020

Contents

Introduction

Carbon-based systems are of great interest in physics, because of the possibility of having a huge number of different structures with a large variety of physical properties. These properties are often linked to the dimensionality of the structures. Among the systems composed only by carbon atoms, graphene is one of the most studied.
Graphene is a two-dimensional material where carbon atoms are arranged in a honeycomb lattice. Experimentally graphene can be isolated starting from the graphite, a three-dimensional carbon allotrope. Graphite is composed by stacked graphene layers kept together by van der Waals forces. Although graphite has been known since about 1564, only recently graphene has been isolated out of the graphite stacking. In 2004 Novoselov, Geim et al. [1], managed to do that and for that reason and for their studies on monolayer graphene they were awarded the Nobel prize in 2010. Since then, graphene has been the topic of many experimental and theoretical studies on its mechanical and transport properties.
Some peculiar properties are its high electron mobility, and its high conductivity, together with its gapless band structure and its mechanical strength and flexibility. The latter property is due to the fact that the sp^2 hybridization between one s orbital and two p orbitals leads to a trigonal planar structure with the formation of a σ bond between carbon atoms, which is responsible for the robustness of the lattice structure in all carbon allotropes. The theoretical interest on graphene is motivated by the peculiar low energy limit of the system, described by a Dirac hamiltonian, namely, the low energy excitations are massless Dirac fermions. This fact is of great importance because the physics emerging from that is the same of that for relativistic massless fermions, with the only difference that, in graphene, Dirac fermions move with a velocity that is lower than the speed of light (about 300 times lower than c).
Relativistic fermions have different properties with respect to those of non-

relativistic ones, which can now be experimentally verified in a condensed matter setting provided by graphene structures. An example is the so-called *Klein paradox* [2], that is related to the difficulty in confining Dirac fermions by an external potential, getting even perfect transmission across potential barriers. Another peculiar effect is the anomalous integer quantum Hall effect, measured experimentally [3], which is the characteristic feature of a monolayer graphene. In addition to this theoretical and experimental studies on the single layer graphene, in the last few years, attention is growing on the so called *van der Waals heterostructures*, which consist of vertically stacked two-dimensional layers held together by the van Der Waals forces. This interest regards also graphene, with the study and realization of multilayered structured.

In this thesis we will focus on the study of a two-layer graphene system, where a small relative rotation is applied. This system is called *twisted bilayer graphene*, tBLG. In the last ten years many experimental works have shown that by twisting two layers of graphene by small angles, one can enhance the conducting properties of the system. Moreover at some specific angles, called *magic angles*, the lowest energy band turns to be very close to the Fermi level and becomes extremely flat. This is of particular interest in the presence of ordered phases of matter like superconductivity. The densities of charge carriers is orders of magnitude lower than the typical two-dimensional superconductors and the measured critical temperature is however relatively high. This makes tBLG a strong coupling superconductor. The great advantage in tBLG with respect to other systems is the simple and fine tunability of carrier densities, magnetic field and temperature, that enables a complete and fine investigation of the rich phase diagram of such a strongly correlated system. Also the interlayer interactions can be fine-tuned by the modulation of the twist angle and/or the application of perpendicular electric fields and of uniaxial strain induced by non hydrostatic pressure [9].

In this work we study the tight binding model for the tBLG, which, in the continuum limit, correctly predicts the presence of angles at which the Fermi velocity vanishes, and, therefore, the presence of flat bands near these magic angles. In particular, we show how, in the low energy limit, one gets an analytical expression for the first magic angle, rederiving the effective model and providing all the details useful for the calculation skipped in literature. Moreover we perform the numerical calculation in order to obtain the full spectrum and the bandwidth for the lowest energy band. The latter result is useful for us when considering the interacting system. In the presence of electron-electron attractive interaction mediated by the phonons the system seems to sustain a superconducting phase. By means of a path integral approach we finally derive the corresponding critical temperature.

Tight Binding model

2.1 First Quantization formulation

To study many body problems one should write the N-body general wavefunction and solve the Schrödinger equation for it. However this is not a directly affordable approach neither analytically nor numerically due to the dimension of the many body wavefunction. In fact, if we think of its generic form, the state of the system can be written as

$$|\Psi\rangle = \sum_{\sigma_1,...,\sigma_N} c_{\sigma_1,...\sigma_N} |\sigma_1, ...\sigma_N\rangle \tag{2.1}$$

where $|\sigma_1, ...\sigma_N\rangle$ is a generic base vector of the Hilbert space $\mathbb{H}^d \otimes ... \otimes \mathbb{H}^d$, where Ψ live, with $\mathbb{H}^d$ space of single particle. The coefficients $c_{\sigma_1,...\sigma_N}$ can be represented as a N-rank tensor, and its dimension grows exponentially with the increasing number of particle in the system. This lead to the impossibility of using such a description to attack a many body problem. In the contest of solid state physics there are different approaches that can be used to simplify the discussion and make the problem treatable. Since our aim is to describe electrons in a solid, we will focus on the band structure theory, in particular on the tight binding method.

An ideal solid is characterized by perfect translational symmetry and infinite size. So for our discussion we think to solids as perfect infinite crystals. In a crystal atoms are disposed on a lattice. The lattice is characterized by a translational symmetry which can be exploited in our description introducing the lattice vector, which is a linear combination of the basis vector of the crystal and describe the infinite translational invariance. To the lattice vector is associated a counterpart in the momentum space, the reciprocal lattice vector, which describes the periodicity of the crystal in the momentum space.

Since our aim is to describe real solids, that have a finite extension, one can overcome this problem introducing the *periodic boundary condition*, that let us describe finite size crystal and bring a discretization in the momentum space. To continue with our aim of finding a model for describing electron in crystals, one has to introduce some approximation. The most important approximation that we introduce is the Born-Oppenheimer approximation. This is based on the idea that the motion of the atoms can be decoupled from the one of the electrons, and this because the electrons are much faster than the atoms, and basically see the atoms in the lattice as frozen, in first approximation (this approximation can be improved in a second moment by adding to the description the scattering of the electrons with the phonons).

With this approximation one describes the motion of the lattice with the harmonic theory, i.e. the lattice can be described as decoupled harmonic oscillators, and its excitations are the so called phonons. For accounting the electrons motion and their excitations instead one can use the band theory, which is based on two important ingredients: the Bloch theorem that is linked to the fact that the electronic wavefunction reflects in a sense the same periodicity of the lattice; and the description of the medium in which the electrons are immersed by the use of a background periodic potential, so that the electronic Hamiltonian of the system can be written as

$$\hat{H} = \hat{H}_e + \hat{V} \tag{2.2}$$

with $\hat{V} = V(\mathbf{r}) = V(\mathbf{r} + \mathbf{R})$ that has the same periodicity of the lattice. In this hamiltonian we see that no interacting potential between electrons is added, because in first approximation we neglect it. This might appear as a strong assumption, but can be justified by the effect of screening of the positive charge surroundings the electrons. In fact the effect of the surrounding positive charge is that of changing the potential generated from the negative charge reducing it to a short-range Yukawa potential, negligible at length larger than the lattice constant, so basically each electron does not feel the presence of other electrons. This is the general hamiltonian and approach of the band theory, but we are interested in a system with a strong binding between atoms and their electrons. This means that we think to a problem in which for each site of the lattice the electron feels basically the potential of the single atom in which is located, and the difference caused by the presence of the other surrounding atoms can be described as a small perturbation. So we use a potential of the form

$$V(\mathbf{r}) = V_{atomic}(\mathbf{r}) + \Delta U(\mathbf{r}), \tag{2.3}$$

decomposed in $V_{atomic}(\mathbf{r})$, i.e. the potential describing the system as isolated atom in the lattice, and $\Delta U(\mathbf{r})$ the term that describes the differences in

energy due of the presence of the other atoms. To give a reason why we are writing the potential in this way one can think at the two opposite situation: if we think to a system made of separated atoms, every atoms has its own electrons localized around its position. If now we think to the atoms in a solid the electrons feels the potential of their atom, but now the presence of the other atoms in the lattice perturbs the potential in which they are immersed. Since we are thinking to a tight-binding model, we can think that each electron is described by a wavefunction that is strongly localized around its own atom, and this means that wavefunction tails go rapidly to zero in a distance of the order of the lattice constant. This is the reason why we think to this perturbation as a small term ΔU, which contains all the corrections to the atomic potential to represent the full periodic lattice potential. For this reason it also makes sense to think at the electrons wavefunction as still localized around its atom also in this case, but the perturbation modifies the system in a way that the wavefunction of the system is not anymore the eigenstate of the single atom hamiltonian, so we can think to the wavefunction as a linear combination of the form

$$\psi(\mathbf{r}) = \sum_{\mathbf{R}} c_{\mathbf{R}} \tilde{\phi}(\mathbf{r} - \mathbf{R}) \tag{2.4}$$

where $\tilde{\phi}(\mathbf{r})$ not necessarily an exact atomic stationary-state wavefunction. Given now $\phi_n(\mathbf{r})$

$$\hat{H}_{at} \left|\phi_n\right\rangle = E_n \left|\phi_n\right\rangle \tag{2.5}$$

eigenstate of the single atom problem, if we think that $\Delta U \phi_n(\mathbf{r})$ is small, as we suppose in our model, we might expect that $\tilde{\phi}(\mathbf{r})$ is not too far form the solution of 2.5, for this reason we think that it might be a combination of a small number of atomic orbitals

$$\tilde{\phi}(\mathbf{r}) = \sum_{n} b_n \phi_n(\mathbf{r}) \tag{2.6}$$

So the general state of the system can be written as

$$\psi(\mathbf{r}) = \sum_{n} b_n \sum_{\mathbf{R}} c_{\mathbf{R}} \phi_n(\mathbf{r} - \mathbf{R}). \tag{2.7}$$

We note that our state must be periodic, with the same periodicity of the lattice, so it has to satisfy the Bloch theorem, and imposing this requirement

we find the form for $c_{\mathbf{R}}$

$$\begin{aligned}
\psi(\mathbf{r}+\mathbf{R}') &= e^{i\mathbf{k}\cdot\mathbf{R}'}\psi(\mathbf{r}) \quad \text{Bloch theorem} \\
&= e^{i\mathbf{k}\cdot\mathbf{R}'}\sum_{\mathbf{R}} c_{\mathbf{R}}\tilde{\phi}(\mathbf{r}+\mathbf{R}'-\mathbf{R}) \\
&= \sum_{\mathbf{R}} e^{i\mathbf{k}\cdot\mathbf{R}'} c_{\mathbf{R}}\tilde{\phi}(\mathbf{r}+\mathbf{R}'-\mathbf{R}) \\
&= \sum_{\mathbf{R}} \tilde{c}_{\mathbf{R}}\tilde{\phi}(\mathbf{r}+\mathbf{R}'-\mathbf{R}) \\
&\Rightarrow \tilde{c}_{\mathbf{R}} = e^{i\mathbf{k}\cdot\mathbf{R}'} c_{\mathbf{R}}
\end{aligned} \tag{2.8}$$

and since for $\mathbf{R}' = 0 \Rightarrow c_{\mathbf{R}} = 1$ to satisfy the general form of $\psi(\mathbf{r})$ and the Bloch theorem we must have $\tilde{c}_{\mathbf{R}} = e^{i\mathbf{k}\cdot\mathbf{R}}$, and so we can write our states as

$$\psi(\mathbf{r}) = \sum_n b_n \sum_{\mathbf{R}'} e^{i\mathbf{k}\cdot\mathbf{R}}\phi_n(\mathbf{r}-\mathbf{R}). \tag{2.9}$$

Using this state we can write the Schrödinger equation for our system

$$\left(\hat{H}_{at} + \Delta\hat{U}\right)|\psi\rangle = \varepsilon_{\mathbf{k}}|\psi\rangle \tag{2.10}$$

Now multiplying this equation by the atomic eigenstate ϕ_m^* both side and integrating, we obtain

$$\int d\mathbf{r}\phi_m^*(\mathbf{r})H_{at}\psi(\mathbf{r}) + \int d\mathbf{r}\phi_m^*(\mathbf{r})\Delta U\psi(\mathbf{r}) = \int d\mathbf{r}\phi_m^*(\mathbf{r})\varepsilon_{\mathbf{k}}\psi(\mathbf{r}). \tag{2.11}$$

Noting that

$$\int d\mathbf{r}\phi_m^*(\mathbf{r})H_{at}\psi(\mathbf{r}) = E_m\int d\mathbf{r}\phi_m^*(\mathbf{r})\psi(\mathbf{r}) \tag{2.12}$$

we arrive to

$$(\varepsilon_{\mathbf{k}} - E_m)\int d\mathbf{r}\phi_m^*(\mathbf{r})\psi(\mathbf{r}) = \int d\mathbf{r}\phi_m^*(\mathbf{r})\Delta U\psi(\mathbf{r}). \tag{2.13}$$

Using now 2.9 in the last equation,and exploiting the orthonormality of the eigenstates of H_{at}, i.e.

$$\int d\mathbf{r}\phi_m^*(\mathbf{r})\phi_n(\mathbf{r}) = \delta_{m,n} \tag{2.14}$$

we arrive finally to an eigenvalue equation that determine the coefficients b_n and the Bloch energies $\varepsilon_{\mathbf{k}}$

$$\begin{aligned}(\varepsilon_{\mathbf{k}} - E_m)b_m = &- (\varepsilon_{\mathbf{k}} - E_m)\sum_n \left(\sum_{\mathbf{R}\neq 0} e^{i\mathbf{k}\cdot\mathbf{R}} \underbrace{\int d\mathbf{r}\phi_m^*(\mathbf{r})\phi_n(\mathbf{r}-\mathbf{R})}_{(1)}\right) b_n + \\ &+ \sum_n \left(\underbrace{\int d\mathbf{r}\phi_m^*(\mathbf{r})\Delta U(\mathbf{r})\phi_n(\mathbf{r})}_{(2)}\right) b_n + \\ &+ \sum_n \left(\sum_{\mathbf{R}\neq 0} e^{i\mathbf{k}\cdot\mathbf{R}} \underbrace{\int d\mathbf{r}\phi_m^*(\mathbf{r})\Delta U(\mathbf{r})\phi_n(\mathbf{r}-\mathbf{R})}_{(3)}\right) b_n\end{aligned} \tag{2.15}$$

and to simplify the notation we can define some quantities starting from $(1), (2), (3)$

$$\begin{aligned}&(1) \quad \int d\mathbf{r}\phi_m^*(\mathbf{r})\phi_n(\mathbf{r}-\mathbf{R}) = \alpha_{m,n}(\mathbf{R}) \\ &(2) \quad \int d\mathbf{r}\phi_m^*(\mathbf{r})\Delta U(\mathbf{r})\phi_n(\mathbf{r}) = \beta_{m,n} \\ &(3) \quad \int d\mathbf{r}\phi_m^*(\mathbf{r})\Delta U(\mathbf{r})\phi_n(\mathbf{r}-\mathbf{R}) = \gamma_{m,n}(\mathbf{R})\end{aligned} \tag{2.16}$$

and so we can rewrite our eigenvalues problem for the tight-binding model as

$$(\varepsilon_{\mathbf{k}} - E_m)b_m = \sum_n \left[-(\varepsilon_{\mathbf{k}} - E_m)\sum_{\mathbf{R}\neq 0}\left(e^{i\mathbf{k}\cdot\mathbf{R}}\alpha_{m,n}(\mathbf{R}) + \gamma_{m,n}(\mathbf{R})\right) + \beta_{m,n}\right] b_n \tag{2.17}$$

2.1.1 Comment on the result

If the problem can be described with the use of only the *s-wave* contribution of the atomic orbital, Eq. (2.17) becames a single equation, which can be recasted in the form

$$\varepsilon_{\mathbf{k}} = E_s + \frac{\beta + \sum_{\mathbf{R}\neq 0} e^{i\mathbf{k}\cdot\mathbf{R}}\gamma(\mathbf{R})}{1 + \sum_{\mathbf{R}\neq 0} e^{i\mathbf{k}\cdot\mathbf{R}}\alpha(\mathbf{R})} \tag{2.18}$$

with

$$\begin{aligned}\beta &= \int d\mathbf{r}|\phi_s(\mathbf{r})|^2\Delta U(\mathbf{r}) \\ \alpha(\mathbf{R}) &= \int d\mathbf{r}\phi_s^*(\mathbf{r})\phi_s(\mathbf{r}-\mathbf{R}) \\ \gamma(\mathbf{R}) &= \int d\mathbf{r}\phi_s^*(\mathbf{r})\Delta U(\mathbf{r})\phi_s(\mathbf{r}-\mathbf{R}).\end{aligned} \tag{2.19}$$

If instead one is interested in bands generated from degenerate atomic orbitals, for example p-wave that are triple degenerate, Eq. (2.17) would give a set of three homogeneous equation, whose eigenvalues are the $\varepsilon_{\mathbf{k}}$ for the three degenerate p-bands, and with the correct coefficients b_n that give the appropriate linear combination. So in the general case one have to solve a $N \times N$ secular problem with N the degeneracy of the considered orbitals. In the case of hybridization, i.e. when one considers a wavefunction composed by mixed orbitals, the dimension of the secular equation becomes the sum of the number of considered states multiplied by their degeneracy.

2.2 Second Quantization formulation

In the second quantization formalism any fermionic single particle operators can be written as

$$A = \sum_{i,j} \langle i|\, \hat{A}\, |j\rangle c_i^\dagger c_j \tag{2.20}$$

where i, j are quantum numbers of the studied system and $c^\dagger, c$ are the fermionic creation and annihilation operators, i.e. they anticommute $\{c_i, c_j^\dagger\} = \delta_{i,j}$, and $|i/j\rangle$ are the generic states of the system describing the state labeled by the i/j quantum number.

If we consider the hamiltonian of our system of non interacting electrons in a crystal we can write it as

$$H = \sum_{i,j} \langle i|\, \hat{H}\, |j\rangle\, c_i^\dagger c_j \tag{2.21}$$

using the same hamiltonian seen in (2.2) with potential (2.3) we can rewrite it as

$$H = \sum_i \langle i|\, \hat{H}_{at}\, |i\rangle\, \hat{N}_i + \sum_{i\neq j} \langle i|\, \Delta\hat{U}\, |j\rangle\, c_i^\dagger c_j + \sum_{i\neq j} \langle j|\, \Delta\hat{U}\, |i\rangle\, c_j^\dagger c_i \tag{2.22}$$

with $\hat{N}$ the number operator, and if we consider $|i,j\rangle$ to be the electronic states of the system, the Wannier functions. Calling now $\langle i|\,\hat{H}_{at}\,|i\rangle = \varepsilon_{at}$ and $-\langle i|\,\Delta\hat{U}\,|j\rangle = t$, we write

$$H = \mathbb{1}\varepsilon_{at} - t\sum_{i\neq j} c_i^\dagger c_j - t\sum_{i\neq j} c_j^\dagger c_i \tag{2.23}$$

where the second term and the third terms are called *hopping terms* Without loss of generality we can put the first term to zero so that all the bands are computed choosing as the zero level the Fermi energy of the system. Our tight-binding hamiltonian in second quantization, adopting also the approximation of keeping only the nearest neighbor hopping terms, can be written as

$$H = -t\sum_{\langle i,j\rangle}\Big(c_i^\dagger c_j + c_j^\dagger c_i\Big). \tag{2.24}$$

where $\langle i,j\rangle$ refers to i,j nearest-neighbors. To adapt this description to systems with more than one atoms in their unitary cell, as in the case of graphene, we can introduce different names for the fermionic operators of different sublattices. For example in a bipartite system with sublattices of type A and B we can call fermionic operator for sites A with a, and for sites B with b, so that

$$H = -t\sum_{\langle i,j\rangle}\Big(a_i^\dagger b_j + b_j^\dagger a_i\Big) \tag{2.25}$$

since nearest neighbor of a site A belongs to the sublattice B and viceversa.

Graphene

3.1 Description and main features

We start now our work by first introducing the general features of a graphene monolayer. In graphene, due to the $s - p^2$ hybridization, the carbon atoms arrange themselves in a honeycomb structure, with an inter atomic distance of $a_0 \simeq 1.42$Å. This lattice is not strictly a Bravais lattice, but it can be thought as an hexagonal Bravais lattice, with lattice constant $a = \sqrt{3}a_0 \simeq 2.46$Å, with a two-atom basis. So for our description we will think at graphene as formed by two sublattices, one for each atom in the basis, that we call sublattice A and sublattice B. In figure 5.1(a) we show the lattice and we highlight the different sublattices by coloring them with different colors. We report the primitive vectors and the basis vectors, showing that for our description we choose to put the origin centered on an atom of type A

$$\mathbf{a}_1 = \frac{a_0}{2}\begin{pmatrix} 3 \\ \sqrt{3} \end{pmatrix}, \mathbf{a}_2 = \frac{a_0}{2}\begin{pmatrix} 3 \\ -\sqrt{3} \end{pmatrix}, \boldsymbol{\tau}_A = \begin{pmatrix} 0 \\ 0 \end{pmatrix}, \boldsymbol{\tau}_B = a_0\begin{pmatrix} -1 \\ 0 \end{pmatrix} \tag{3.1}$$

From this definition of the primitive vectors, we can define the primitive vectors of the reciprocal lattice using

$$\mathbf{a}_i \cdot \mathbf{b}_j = 2\pi\delta_{i,j} \tag{3.2}$$

and so the primitive vectors of the reciprocal lattice are

$$\mathbf{b}_1 = \frac{2\pi}{3a_0}\begin{pmatrix} 1 \\ \sqrt{3} \end{pmatrix}, \mathbf{b}_2 = \frac{2\pi}{3a_0}\begin{pmatrix} 1 \\ -\sqrt{3} \end{pmatrix}. \tag{3.3}$$

From all the points in the first Brillouin zone, graphene have two high symmetry points, called *Dirac points* for reasons that will be explained in the

following chapters, that have a correspondence with their symmetric counterpart with respect to the Γ point. Since their coordinates are needed we will report them here

$$\mathbf{K} = \frac{2\pi}{3\sqrt{3}a_0}\begin{pmatrix}\sqrt{3}\\1\end{pmatrix}, \mathbf{K}' = \frac{2\pi}{3\sqrt{3}a_0}\begin{pmatrix}\sqrt{3}\\-1\end{pmatrix}. \tag{3.4}$$

The first Brillouin zone with its primitive vectors and Dirac points are represented in Fig. 5.1(b).

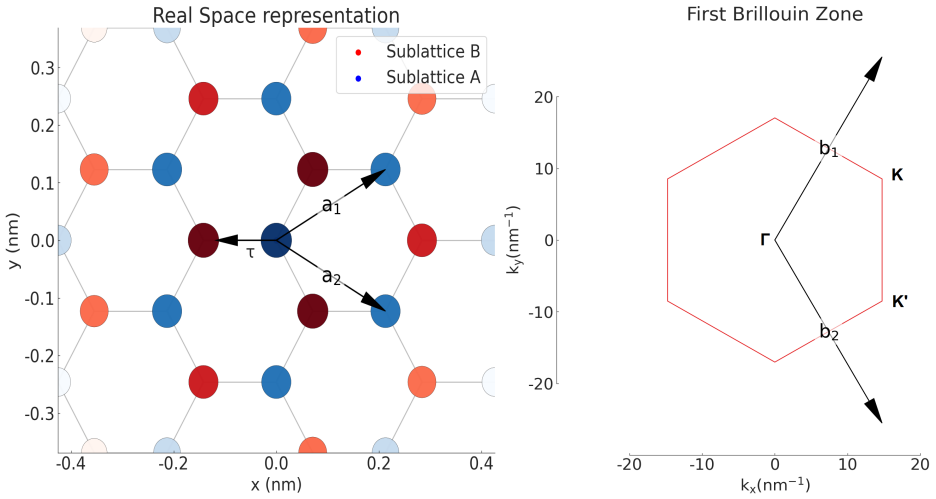

(a) (b)

Figure 3.1: Real Space (a) and First Brillouin zone (b) representations

3.2 Tight-Binding approach

To study the graphene properties, a low energy model can be derived for the generic tight binding approach. So we start writing the Hamiltonian in second quantization in the case of a tight binding contribution

$$H = -t \sum_{\langle i,j\rangle,\sigma} \left(a^\dagger_{i,\sigma} b_{j,\sigma} + b^\dagger_{j,\sigma} a_{i,\sigma} \right) - t' \sum_{\langle\langle i,j\rangle\rangle,\sigma} \left(a^\dagger_{i,\sigma} a_{j,\sigma} + b^\dagger_{i,\sigma} b_{j,\sigma} \right) \tag{3.5}$$

where we denote with $a(\mathbf{R}_i) = a_i$ the field operator for an electron in a sublattice of type A in position $\mathbf{R}_i$, and the same for b but for B sublattice. With $\langle i,j\rangle$ we refer to first nearest neighbors and $\langle\langle i,j\rangle\rangle$ to second nearest neighbors. As we see in the general description of the previous chapter, if we consider a site of type A, the first n.n. are the B atoms surrounding it, as can be seen from figure 3.2, and have coordinates denoted by the vectors $\boldsymbol{\delta}_i$, $i = 1,2,3$. We write the field operators in a momentum basis

$$\begin{aligned} a_i &= \frac{1}{\Omega} \sum_{\mathbf{k}} e^{-i\mathbf{k}\cdot\mathbf{R}_i} a(\mathbf{k}) \\ b_j &= \frac{1}{\Omega} \sum_{\mathbf{k}} e^{-i\mathbf{k}\cdot(\mathbf{R}_j+\boldsymbol{\tau})} b(\mathbf{k}) \end{aligned} \tag{3.6}$$

using this representation in hamiltonian (3.5) we can write

$$\begin{aligned} H = &-\frac{t}{\Omega'} \sum_{\langle i,j\rangle,\sigma} \sum_{\mathbf{k},\mathbf{k}'} \left[e^{i\mathbf{k}\cdot\mathbf{R}_i} a^\dagger(\mathbf{k}) e^{-i\mathbf{k}'\cdot(\mathbf{R}_j+\boldsymbol{\tau})} b(\mathbf{k}') + e^{i\mathbf{k}'\cdot(\mathbf{R}_j+\boldsymbol{\tau})} b^\dagger(\mathbf{k}') e^{-i\mathbf{k}\cdot\mathbf{R}_i} a(\mathbf{k}) \right] + \\ &- \frac{t'}{\Omega'} \sum_{\langle\langle i,j\rangle\rangle,\sigma} \sum_{\mathbf{k},\mathbf{k}'} \left[e^{i\mathbf{k}\cdot\mathbf{R}_i} a^\dagger(\mathbf{k}) e^{-i\mathbf{k}'\cdot\mathbf{R}_j} a(\mathbf{k}') + e^{i\mathbf{k}'\cdot(\mathbf{R}_i+\boldsymbol{\tau})} b^\dagger(\mathbf{k}') e^{-i\mathbf{k}\cdot(\mathbf{R}_j+\boldsymbol{\tau})} b(\mathbf{k}) \right] \end{aligned} \tag{3.7}$$

To proceed we have to specify $\langle i,j\rangle$ and $\langle\langle i,j\rangle\rangle$, i.e. the nearest neighbor and next nearest neighbor coordinates. If we are centered in a sublattice A the n.n. are all the adjacent B sites, and vice versa. So by writing explicitly $\boldsymbol{\delta}_j$, (see Fig. 3.2), the sum over j becomes a sum over $\boldsymbol{\delta}$. The second n.n. are the sublattice of the same type, and they differs by a lattice vector, so the sum

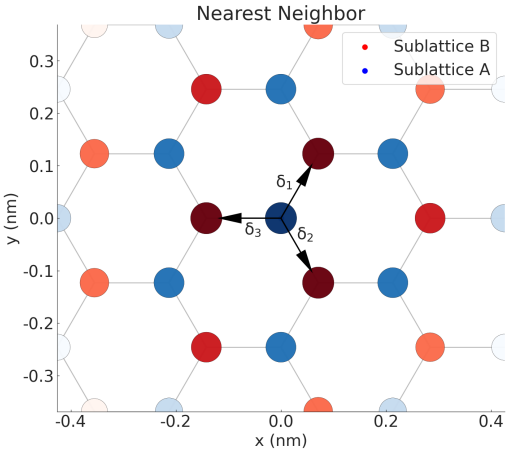

$$\boldsymbol{\delta}_1 = \frac{a_0}{2}\begin{pmatrix}1\\ \sqrt{3}\end{pmatrix}$$
$$\boldsymbol{\delta}_2 = \frac{a_0}{2}\begin{pmatrix}1\\ -\sqrt{3}\end{pmatrix} \tag{3.8}$$
$$\boldsymbol{\delta}_3 = a_0\begin{pmatrix}-1\\ 0\end{pmatrix}$$

Figure 3.2

over the $\langle\langle i,j\rangle\rangle$ gives a delta function. So Eq. (3.7) becomes

$$\begin{aligned}
&= -\frac{t}{\Omega'}\sum_{\mathbf{k},\mathbf{k}'}\sum_{i,\boldsymbol{\delta},\sigma}\left[e^{i(\mathbf{k}-\mathbf{k}')\cdot\mathbf{R}_i}e^{-i\mathbf{k}'\cdot\boldsymbol{\delta}}a^\dagger(\mathbf{k})b(\mathbf{k}') + e^{i\mathbf{k}'\cdot\boldsymbol{\delta}}e^{-i(\mathbf{k}-\mathbf{k}')\cdot\mathbf{R}_i}b^\dagger(\mathbf{k}')a(\mathbf{k})\right] + \\
&- \frac{t'}{\Omega'}\sum_{\mathbf{k},\sigma}\left[a^\dagger(\mathbf{k})a(\mathbf{k}) + b^\dagger(\mathbf{k})b(\mathbf{k})\right] = \\
&\downarrow \ \tfrac{1}{\Omega'}\textstyle\sum_i e^{i(\mathbf{k}-\mathbf{k}')\cdot\mathbf{R}_i} = \delta_{\mathbf{k},\mathbf{k}'} \\
&= -t\sum_{\mathbf{k},\boldsymbol{\delta},\sigma}\left[e^{-i\mathbf{k}\cdot\boldsymbol{\delta}}a^\dagger(\mathbf{k})b(\mathbf{k}) + e^{i\mathbf{k}\cdot\boldsymbol{\delta}}b^\dagger(\mathbf{k})a(\mathbf{k})\right] - t'\sum_{\mathbf{k},\sigma}\left[a^\dagger(\mathbf{k})a(\mathbf{k}) + b^\dagger(\mathbf{k})b(\mathbf{k})\right]
\end{aligned} \tag{3.9}$$

where in the last step we sum over $\mathbf{k}'$ exploiting the $\delta_{\mathbf{k},\mathbf{k}'}$. Introducing the spinor $\Psi_{\mathbf{k}} = \begin{pmatrix}a(\mathbf{k})\\ b(\mathbf{k})\end{pmatrix}$ we can write (3.9) in the following matrix form

$$H = \sum_{\mathbf{k}} \Psi^\dagger_{\mathbf{k}} h(\mathbf{k}) \Psi_{\mathbf{k}} \tag{3.10}$$

where $h(\mathbf{k}) = -\begin{pmatrix}t' & t\Delta_{\mathbf{k}}\\ t\Delta^*_{\mathbf{k}} & t'\end{pmatrix}$ and $\Delta_{\mathbf{k}} = \sum_{\boldsymbol{\delta}} e^{i\mathbf{k}\cdot\boldsymbol{\delta}}$.

Since we are interested in the low energy limit and $t' \ll t$ [1], we can neglect

[1] We refer to the result of [13] where they show using *ab initio* calculation that $0.02t < t' < 0.2t$

for our purposes the second n.n. contribution, and this leads to

$$h(\mathbf{k}) = -\begin{pmatrix} 0 & t\Delta_{\mathbf{k}} \\ t\Delta_{\mathbf{k}}^* & 0 \end{pmatrix}. \tag{3.11}$$

The hamiltonian found in this way can also be expressed in a more compact way using the Pauli matrices. This can be done by writing the complex number $e^{i\mathbf{k}\cdot\boldsymbol{\delta}}$ using the Euler's formula, $e^{i\mathbf{k}\cdot\boldsymbol{\delta}} = \cos(\mathbf{k}\cdot\boldsymbol{\delta}) + i\sin(\mathbf{k}\cdot\boldsymbol{\delta})$, so that we can write

$$\begin{aligned} h(\mathbf{k}) &= -t\sum_{\delta}\begin{pmatrix} 0 & \cos(\mathbf{k}\cdot\boldsymbol{\delta}) + i\sin(\mathbf{k}\cdot\boldsymbol{\delta}) \\ \cos(\mathbf{k}\cdot\boldsymbol{\delta}) - i\sin(\mathbf{k}\cdot\boldsymbol{\delta}) & 0 \end{pmatrix} = \\ &= -t\sum_{\delta}\cos(\mathbf{k}\cdot\boldsymbol{\delta})\sigma_x - sin(\mathbf{k}\cdot\boldsymbol{\delta})\sigma_y. \end{aligned} \tag{3.12}$$

3.2.1 Hamiltonian in proximity of the Dirac Points

If we now focus our attention near the K-points, we find a Dirac like equation. To see this we first change notation in order to express all the momenta with respect to these Dirac points whose coordinates are reminded here

$$\mathbf{K} = \frac{2\pi}{3\sqrt{3}a_0}\begin{pmatrix}\sqrt{3}\\1\end{pmatrix}, \mathbf{K}' = \frac{2\pi}{3\sqrt{3}a_0}\begin{pmatrix}\sqrt{3}\\-1\end{pmatrix} \tag{3.13}$$

We will use in the derivation only one of these two points, since the same result could be obtain using the other one. We express the momenta introducing $\mathbf{q} = \mathbf{k} - \mathbf{K}$, so our $\Delta_{\mathbf{k}} = \Delta_{\mathbf{q}+\mathbf{K}} = \sum_{\boldsymbol{\delta}} e^{i(\mathbf{q}+\mathbf{K})\cdot\boldsymbol{\delta}}$. Substituting the coordinates of $\boldsymbol{\delta}$ and of $\mathbf{K}$ we can rewrite $\Delta_{\mathbf{q}+\mathbf{K}}$ as follows

$$\begin{aligned} \Delta_{\mathbf{q}+\mathbf{K}} &= \sum_{\boldsymbol{\delta}} e^{i(\mathbf{q}+\mathbf{K})\cdot\boldsymbol{\delta}} = \\ &= e^{i\frac{a_0}{2}(q_x+K_x)+i\frac{\sqrt{3}}{2}a_0(q_y+K_y)} + e^{i\frac{a_0}{2}(q_x+K_x)-i\frac{\sqrt{3}}{2}a_0(q_y+K_y)} + e^{-i(q_x+K_x)a_0} = \\ &= e^{-i(q_x+K_x)a_0}\left\{1 + 2e^{i\frac{3}{2}a_0(q_x+K_x)}\cos\left[\frac{\sqrt{3}}{2}a_0(q_y+K_y)\right]\right\} = \\ &= e^{-i(q_x+K_x)a_0}\left[1 - 2e^{i\frac{3}{2}a_0 q_x}\cos\left(\frac{\sqrt{3}}{2}a_0 q_y + \frac{\pi}{3}\right)\right] = \\ &\Big\downarrow \text{ expanding around } \mathbf{q}\simeq\mathbf{0} \\ &\approx -\frac{3}{2}a_0\theta(q_x + iq_y) \end{aligned} \tag{3.14}$$

where we called $\theta = ie^{-iK_x a_0}$. Since θ is only a phase it can be incorporated in the spinors and can be omitted since the phase of the wavefunctions does not change the physics. Finally we have

$$h(\mathbf{K}) \simeq v_f \begin{pmatrix} 0 & q_x + iq_y \\ q_x - iq_y & 0 \end{pmatrix} = v_f \boldsymbol{\sigma} \cdot \mathbf{k} \tag{3.15}$$

where $v_f = 3a_0 t/2$, and $\boldsymbol{\sigma} = (\sigma_x, \sigma_y)^T$. In the case of momenta in proximity of the $\mathbf{K}'$ point, the hamiltonian is almost the same $h(\mathbf{K}') = v_f \boldsymbol{\sigma}^* \cdot \mathbf{k}$, with $\boldsymbol{\sigma}^* = (\sigma_x, -\sigma_y)^T$. This is clearly a Dirac like hamiltonian (in momentum space). This shows that near the Dirac points the dispersion relation becomes linear in $|\mathbf{k}|$.

3.3 Energy bands

We can compute the eigenvalues of the hamiltonian (3.10) with only n.n. contributions, that are $E_\pm = \pm t\sqrt{\Delta_{\mathbf{k}} \Delta_{\mathbf{k}}^*}$. Expressing explicitly the $\Delta_{\mathbf{k}}$, using (3.14) (and expanding near $\mathbf{K}$), we obtain

$$E_\pm = \pm t \sqrt{1 + 4\cos\left(\frac{3}{2} a_0 k_x\right) \cos\left(\frac{\sqrt{3}}{2} a_0 k_y\right) + 4\cos^2\left(\frac{\sqrt{3}}{2} a_0 k_y\right)} \tag{3.16}$$

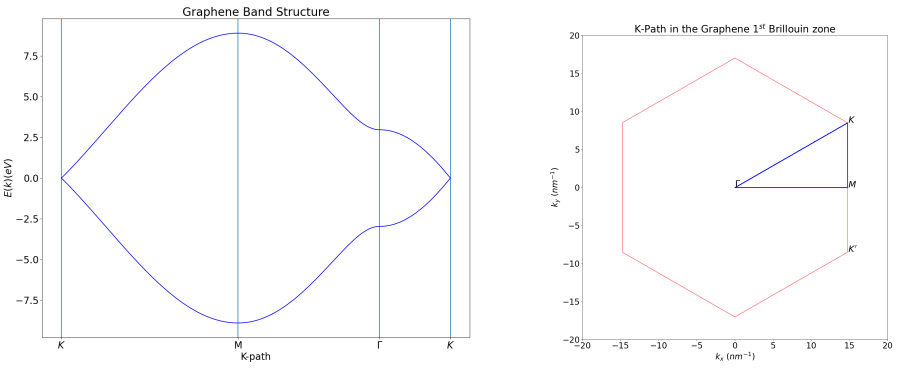

(a) (b)

Figure 3.3: Graphene energy bands: (a) $E(\mathbf{k})$ along the path highlighted in (b)

As one can see from figure 3.3, the Dirac points are the points where the energy becomes null. The bands structure is highly symmetric and the low energy

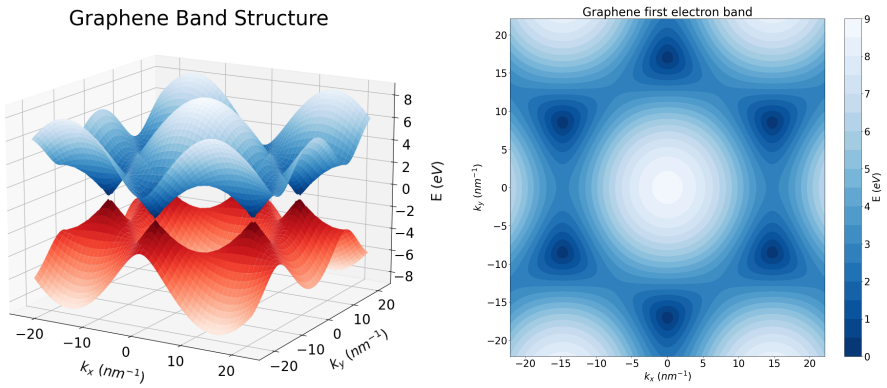

(a) (b)

Figure 3.4: A 3D-plot for graphene low energy spectrum.

spectrum is gapless and has linear behavior near the Dirac points, forming Dirac cones as shown in Fig. 3.4. We finally remind that we have also a spin symmetry to be considered in the model.

Double Layer Graphene

We now extend the description to the double layer. This structure can be obtained experimentally and the typical interlayer distance is equal to $d_\perp = 3.35$Å. When stacking two single layers, it is important to specify in which way the atoms of the first layer are arranged with respect to the other. There can be several kinds of stacking but we mention the two main ones: 1) the AA stacking, that consists in putting the atoms of one layer exactly above the atoms of the second layer; 2) the AB stacking, or Bernal stacking, which consists in putting the atoms of sublattice A of the first layer aligned with the carbon atoms of the sublattice B in the second layer, while the B atoms remain over the center of the hexagon. Experimentally [18] it is found that the AA stacking is metastable while the Bernal-stacked bilayer is stable. We now proceed in studying the electron properties of the Bernal-stacked bilayers.

4.1 Hamiltonian generalization to Bilayer

To construct the model we will use the single layer hamiltonian found in the previous section, and we add the interlayer hopping, using a nearest-neighbor approximation also for this term. The hamiltonian can be written as

$$H = H_1 + H_2 + H_\perp \tag{4.1}$$

where $H_i, i = 1, 2$ are the hamiltonian respectively of the first and second layer and the last term the interlayer hopping. We can write also this term in the second quantization formalism

$$H_\perp = t_\perp \sum_{\mathbf{R}^{(1)},\mathbf{R}^{(2)}} a_1^\dagger(\mathbf{R}^{(1)}) b_2(\mathbf{R}^{(2)} + \boldsymbol{\tau}^2) + b_2^\dagger(\mathbf{R}^{(2)} + \boldsymbol{\tau}^2) a_1(\mathbf{R}^{(1)}) \tag{4.2}$$

where we call

$$\langle \mathbf{R}^{(1)}| \, H_\perp \, |\mathbf{R}^{(2)} + \boldsymbol{\tau}^{(2)}\rangle = \langle \mathbf{R}^{(2)} + \boldsymbol{\tau}^{(2)}| \, H_\perp \, |\mathbf{R}^{(1)}\rangle = t_\perp. \tag{4.3}$$

We can move to the momentum space, by introducing

$$|\Psi^{(l)}_{\mathbf{k},\alpha}\rangle = \frac{1}{\sqrt{N}} \sum_{\mathbf{R}^{(l)}+\boldsymbol{\tau}_\alpha{}^{(l)}} e^{i\mathbf{k}\cdot\left(\mathbf{R}^{(l)}+\boldsymbol{\tau}_\alpha{}^{(l)}\right)} \, |\mathbf{R}^{(l)} + \boldsymbol{\tau}_\alpha{}^{(l)}\rangle \tag{4.4}$$

where $l = 1, 2$ is the layer index and $\alpha = A, B$ the sublattice index. Using the lattice convention adopted for the single layer graphene we have that $\boldsymbol{\tau}_A = (0, 0)^T$ and $\boldsymbol{\tau}_B = (0, -a_0)^T$. By expressing also the fermionic creation and annihilation operators in the momentum space

$$\begin{aligned} \alpha_l(\mathbf{R}^{(l)}) &= \frac{1}{N} \sum_{\mathbf{k}} e^{-i\mathbf{k}\cdot\left(\mathbf{R}^{(l)}+\boldsymbol{\tau}_\alpha{}^{(l)}\right)} \alpha_l(\mathbf{k}) \\ \alpha_l^\dagger(\mathbf{R}^{(l)}) &= \frac{1}{N} \sum_{\mathbf{k}} e^{-i\mathbf{k}\cdot\left(\mathbf{R}^{(l)}+\boldsymbol{\tau}_\alpha{}^{(l)}\right)} \alpha_l^\dagger(\mathbf{k}) \end{aligned} \tag{4.5}$$

with the same indices convention of before, we can write the total hamiltonian of the system in the momentum space as

$$H = \sum_{\mathbf{k}} \Psi^\dagger(\mathbf{k}) H(\mathbf{k}) \Psi(\mathbf{k}) \tag{4.6}$$

where we introduced the spinor $\Psi^\dagger(\mathbf{k}) = \begin{pmatrix} a_1^\dagger(\mathbf{k}) & b_1^\dagger(\mathbf{k}) & a_2^\dagger(\mathbf{k}) & b_2^\dagger(\mathbf{k}) \end{pmatrix}$ and

$$H(\mathbf{k}) = \begin{pmatrix} 0 & -t\Delta_{\mathbf{k}} & 0 & t_\perp \\ -t\Delta^*_{\mathbf{k}} & 0 & 0 & 0 \\ 0 & 0 & 0 & -t\Delta_{\mathbf{k}} \\ t_\perp & 0 & -t\Delta^*_{\mathbf{k}} & 0 \end{pmatrix}. \tag{4.7}$$

4.2 Band Structure

By solving the eigenvalue problem for the hamiltonian $H(\mathbf{k})$, we obtain

$$\begin{aligned} E_{\pm,\pm}(\mathbf{k}) &= \pm t \sqrt{\left(\frac{t_\perp}{2t}\right)^2 + \Delta_{\mathbf{k}}\Delta^*_{\mathbf{k}}} \pm \frac{t_\perp}{2} = \\ &= \pm t \sqrt{\left(\frac{t_\perp}{2t}\right)^2 + 1 + 4\cos\left(\frac{3}{2}ak_x\right)\cos\left(\frac{\sqrt{3}}{2}ak_y\right) + 4\cos^2\left(\frac{\sqrt{3}}{2}ak_y\right)} \pm \frac{t_\perp}{2} \end{aligned} \tag{4.8}$$

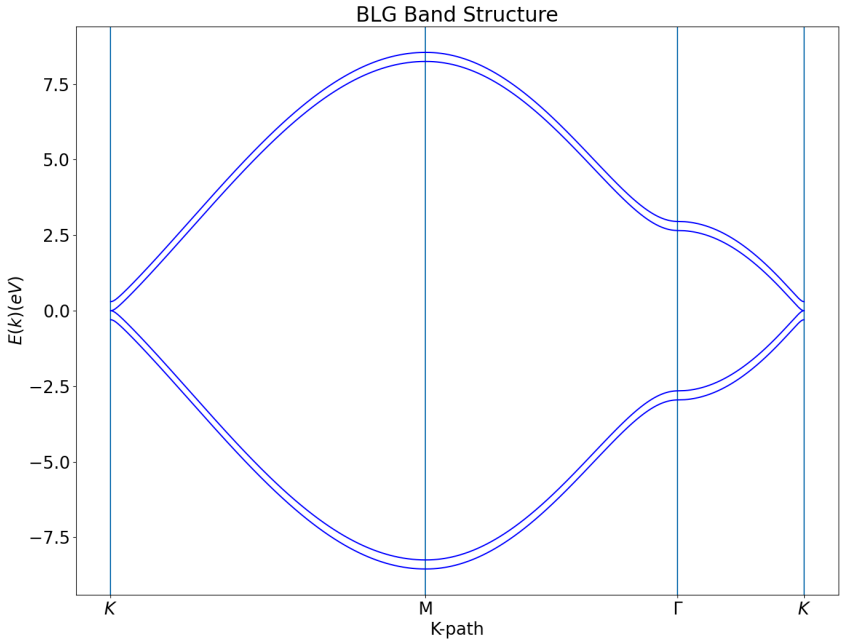

Figure 4.1: BLG band structure

and evaluating along the same path shown in Fig. 3.3 we obtain the band structure depicted in Fig. 4.1. The presence of the hopping term between layers breaks the double degeneracy of the hamiltonian of the two decoupled layers, splitting the top and bottom band in two different bands. Also in this case, the highest hole band and the lowest electron band become gapless in proximity of the Dirac points, as was shown for the single layer graphene.

Twisted Bilayer Graphene

5.1 Moiré Superlattice

The system analyzed is an AB stacking of two graphene layers, to which is applied a small translation vector $\boldsymbol{d}$ and a small rotation θ. We will proceed now in introducing the continuum model, introduced by R. Bistritzer and A. H. MacDonald, [5], to describe the problem and we will refer to this model as *BM model*. Before we start, we remember what is a Moiré pattern which, being the key of the regained periodicity, is of foundamental importance for a tight-binding description. A Moiré pattern is formed when two copies of a periodic structure are overlaid with a relative small twist. This results in a new periodic *superlattice*, as can be seen from figure 5.1. Is important to notice that in general the commensurability of the two layers is dependent on the value of the rotation angle. This observation is important because in general a relative twist of the two layers in a commensurate structure leads to the same crystalline structure (with eventually a rescaling of the unit cell). One has to notice that only a small set of discrete values of the twist angle leads to commensurate structures, in all the other cases of general rotations, greater than few degrees, the periodicity of the crystal is destroyed, resulting in the complete electronic isolation of the two layers. Mathematically this has, as main consequence, the non-applicability of the Bloch's theorem. Instead if the rotation is small, i.e. $\lesssim 10^\circ$, a Moiré pattern is formed and this is the key of the BM model for the tBLG, and leads to the so called *Moiré Bloch bands*. The differences in the patterns obtained by different rotations are shown in figure 5.1: panels a),b),c) show how, for small angles, we obtain commensurate structures, instead as shown by panel d), a large twist angle leads to the destruction of the periodicity.

In the following sections we will see how the superlattice and its Brillouin

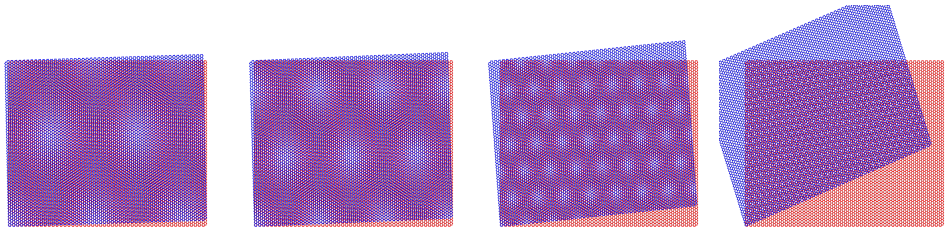

(a) (b) (c) (d)

Figure 5.1: Dependence of Moiré pattern on the twist angle. From left to right: 1.5°, 2.0°, 5.0°, 20.0°

zone, called Moiré Brillouin zone, is introduced and characterized. Let us first introduce the real space and the Moiré Brillouin zone primitive vectors

$$\begin{aligned} \mathbf{b}_1^M &= \frac{\sqrt{3}}{2} k_\theta \begin{pmatrix} 1 \\ -\sqrt{3} \end{pmatrix}, \ \mathbf{b}_2^M = \frac{\sqrt{3}}{2} k_\theta \begin{pmatrix} 1 \\ \sqrt{3} \end{pmatrix} \\ \mathbf{a}_1^M &= \frac{2\pi}{3k_\theta} \begin{pmatrix} \sqrt{3} \\ -1 \end{pmatrix}, \ \mathbf{a}_2^M = \frac{2\pi}{3k_\theta} \begin{pmatrix} \sqrt{3} \\ 1 \end{pmatrix} \end{aligned} \tag{5.1}$$

with $k_\theta = (8\pi \sin(\theta/2))/(3\sqrt{3}a_0)$. In the next section, starting from the tight-binding approach we will derive the continuum model for the tBLG.

5.2 Continuum model for the tBLG

Before we introduce the model let us start defining some quantities. We will call $a = 2.46$Å the lattice constant and $a_0 = a/\sqrt{(3)}$ the carbon-carbon distance. We denote the twist angle with θ. We account the lattice vectors[1] of the two layers as $\mathbf{a}_1^l$,$\mathbf{a}_2^l$, where $l = (1, 2)$ denote the layer index. To these will corresponds two reciprocal lattice vectors $\mathbf{b}_1^l$,$\mathbf{b}_2^l$, and this satisfy the usual relation for the reciprocal lattice vectors, i.e. $\mathbf{b}_a^l \cdot \mathbf{a}_b^l = 2\pi\delta_{a,b}$.

To insert the dependence on the twist angle we split the rotation in half rotation for a layer and half for the other, symmetrizing the notation, and this lead to

[1] We notice that for this section we express the primitive cell basis in a different reference system, with respect to the one used in previous chapters. In this way the computed quantities are easier to express

$$\begin{aligned} \mathbf{a}_1^l &= \frac{\sqrt{3}}{2} a_0 R_{\theta/2}^l \begin{pmatrix} -1 \\ \sqrt{3} \end{pmatrix}, \quad \mathbf{a}_2^l = \frac{\sqrt{3}}{2} a_0 R_{\theta/2}^l \begin{pmatrix} -1 \\ -\sqrt{3} \end{pmatrix} \\ \boldsymbol{\tau}_A^l &= \begin{pmatrix} 0 \\ 0 \end{pmatrix}, \quad \boldsymbol{\tau}_B^l = a_0 R_{\theta/2}^l \begin{pmatrix} 0 \\ -1 \end{pmatrix} \\ \mathbf{b}_1^l &= \frac{2\pi}{3a_0} R_{\theta/2}^l \begin{pmatrix} -\sqrt{3} \\ 1 \end{pmatrix}, \quad \mathbf{b}_2^l = \frac{2\pi}{3a_0} R_{\theta/2}^l \begin{pmatrix} -\sqrt{3} \\ -1 \end{pmatrix} \end{aligned} \tag{5.2}$$

with $l = 1, 2$ layer index, as can be seen in figure 5.2 and with

$$R_{\theta/2}^1 = \begin{pmatrix} \cos(\theta/2) & -\sin(\theta/2) \\ \sin(\theta/2) & \cos(\theta/2) \end{pmatrix}, \quad R_{\theta/2}^2 = \begin{pmatrix} \cos(\theta/2) & \sin(\theta/2) \\ -\sin(\theta/2) & \cos(\theta/2) \end{pmatrix} \tag{5.3}$$

the rotation matrices of angle $\pm\theta/2$ for the two different layers. We will refer to the i-th position on layer l as $\mathbf{R}^{(l)}$ and to it we associate a reciprocal lattice vector $\mathbf{G}^{(l)}$, so that all the position of the atom of a layer can be described in real space by $\mathbf{R}^{(l)} = m\mathbf{a}_1^l + n\mathbf{a}_2^l$ and in the reciprocal space as $\mathbf{G}^{(l)} = k\mathbf{b}_1^l + w\mathbf{b}_2^l$, with $m, n, k, w \; in \mathbb{Z}$.

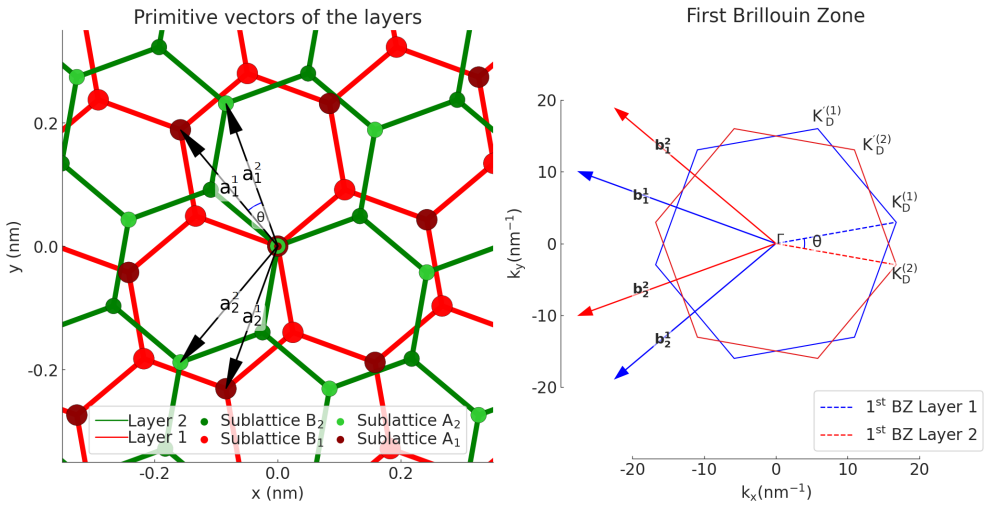

(a) (b)

Figure 5.2: tBLG Real Space and Brillouin Zone representation

The model consist of two single-layer Dirac-Hamiltonian terms derived by the tight-binding approach described in section 1.2 and of a tunneling term,

that describes the inter layers hopping energy contributions. Starting from the single layer energy terms we can adapt the Dirac hamiltonian of the monolayer graphene to our system. After a rotation with respect to a fixed coordinate system we have the Hamiltonian

$$h_{\mathbf{k}}(\theta) = -v|k| \begin{pmatrix} 0 & e^{i(\theta_k - \theta)} \\ e^{-i(\theta_k - \theta)} & 0 \end{pmatrix} \tag{5.4}$$

with $h_k(\theta)$ the Dirac hamiltonian of a single layer, v the Fermi velocity, $\mathbf{k}$ the momentum measured from the layer's Dirac point, θ_k the momentum orientation relative to the x axis. If we consider our symmetric description we can write the hamiltonian of the decoupled two layers as $|1\rangle h(\theta/2) \langle 1| + |2\rangle h(-\theta/2) \langle 2|$, considering the $|l\rangle \langle l|$ the projectors on layer l. For accounting the interlayer hopping, we consider that in general the hopping $t(r)$ is in general a function of the position r. We will assume in Eq. (5.5) the two-center approximation, i.e. that the interlayer hopping is only a function of the two positions. We want to move to the representation in the momentum space, so starting from the tunneling interlayer hamiltonian written in second quantization in real space, we have

$$V_{m,l} = \sum_{\mathbf{R}^{(m)},\alpha,\mathbf{R}^{(l)},\beta} \alpha_m^\dagger(\mathbf{R}^{(m)}) t \left(\mathbf{R}^{(m)} + \boldsymbol{\tau}_\alpha^{(m)} - \mathbf{R}^{(l)} - \boldsymbol{\tau}_\beta^{(l)} \right) \beta_l(\mathbf{R}^{(l)}) \tag{5.5}$$

where α/β are the fermionic operators for the sublattice A or B, m/l layer indices, and we define $t\left(\mathbf{R} + \boldsymbol{\tau}_\alpha - \mathbf{R}' - \boldsymbol{\tau}'_\beta\right)$ as

$$\langle \mathbf{R} + \boldsymbol{\tau}_\alpha | \, H_T \, | \mathbf{R}' + \boldsymbol{\tau}'_\beta \rangle = t\left(\mathbf{R} + \boldsymbol{\tau}_\alpha - \mathbf{R}' - \boldsymbol{\tau}'_\beta\right) \tag{5.6}$$

where $|\mathbf{R} + \boldsymbol{\tau}_\alpha\rangle$ are Wannier functions. For simplicity we fix the indices of the layer, and switching to the momentum space we can write

$$V_{1,2} = \sum_{\mathbf{k},\alpha,\mathbf{p}',\beta} \alpha_1^\dagger(\mathbf{k}) T^{\alpha,\beta}_{\mathbf{k},\mathbf{p}'} \beta_2(\mathbf{p}') \tag{5.7}$$

with

$$T^{\alpha,\beta}_{\mathbf{k},\mathbf{p}'} = \langle \Psi^{(1)}_{\mathbf{k},\alpha} | \, H_T \, | \Psi^{(2)}_{\mathbf{p}',\beta} \rangle \tag{5.8}$$

and

$$\begin{aligned} |\Psi^{(1)}_{\mathbf{k},\alpha}\rangle &= \frac{1}{\sqrt{N}} \sum_{\mathbf{R}^{(1)}} e^{i\mathbf{k}\cdot(\mathbf{R}^{(1)} + \boldsymbol{\tau}_\alpha^{(1)})} \, |\mathbf{R}^{(1)} + \boldsymbol{\tau}_\alpha^{(1)}\rangle \\ |\Psi^{(2)}_{\mathbf{p}',\beta}\rangle &= \frac{1}{\sqrt{N}} \sum_{\mathbf{R}^{(2)}} e^{i\mathbf{p}'\cdot(\mathbf{R}^{(2)} + \boldsymbol{\tau}'_\beta)} \, |\mathbf{R}^{(2)} + \boldsymbol{\tau}_\beta^{(2)}\rangle \end{aligned} \tag{5.9}$$

and we use α, β as sublattice indices, $\mathbf{k}, \mathbf{p}'$ respectively momentum for the first and the second layer.

We derive the general form in the reciprocal lattice space of the $T^{\alpha,\beta}_{\mathbf{k},\mathbf{p}'}$

$$T^{\alpha,\beta}_{\mathbf{k},\mathbf{p}'} = \frac{1}{N} \sum_{\mathbf{R}^{(1)},\mathbf{R}^{(2)}} t\left(\mathbf{R}^{(1)} + \boldsymbol{\tau}^{(1)}_{\alpha} - \mathbf{R}^{(2)} - \boldsymbol{\tau}^{(2)}_{\beta} + \mathbf{d}\right) e^{-i\mathbf{k}\cdot(\mathbf{R}^{(1)}+\boldsymbol{\tau}^{(1)}_{\alpha})+i\mathbf{p}'\cdot(\mathbf{R}^{(2)}+\boldsymbol{\tau}^{(2)}_{\beta})+\mathbf{d}} \tag{5.10}$$

but since $t(\mathbf{R}^{(1)} + \boldsymbol{\tau}^{(1)}_{\alpha} - \mathbf{R}^{(2)} - \boldsymbol{\tau}^{(2)}_{\beta} + \mathbf{d})$ is periodic with respect to $\mathbf{R}^{(1)}$ and $\mathbf{R}^{(2)}$ we can express it as a series in the reciprocal lattice space, i.e.

$$t(\mathbf{R}^{(1)} + \boldsymbol{\tau}^{(1)}_{\alpha} - \mathbf{R}^{(2)} - \boldsymbol{\tau}^{(2)}_{\beta} + \mathbf{d}) \to \sum_{\mathbf{G}^{(1)},\mathbf{G}^{(2)}} t_{\mathbf{G}^{(1)},-\mathbf{G}^{(2)}} \quad e^{i\mathbf{G}^{(1)}\cdot\mathbf{R}^{(1)}} e^{i\mathbf{G}^{(2)}\cdot\mathbf{R}^{(2)}} \tag{5.11}$$

inserting this relation in the previous equation and expressing $\mathbf{R}^{(2)} = \mathbf{R}^{(1)} + \boldsymbol{\tau}^{(1)}_{\alpha} - \boldsymbol{\tau}^{(2)}_{\beta} + \mathbf{d} - \mathbf{r}$, we obtain

$$T^{\alpha,\beta}_{\mathbf{k},\mathbf{p}'} = \frac{1}{N} \sum_{\mathbf{r},\mathbf{R}^{(1)}} \sum_{\mathbf{G}^{(1)},\mathbf{G}^{(2)}} t_{\mathbf{G}^{(1)},-\mathbf{G}^{(2)}} \quad e^{i\mathbf{G}^{(1)}\cdot\mathbf{R}^{(1)}} e^{i\mathbf{G}^{(2)}\cdot(\mathbf{R}^{(1)}+\boldsymbol{\tau}^{(1)}_{\alpha}-\boldsymbol{\tau}^{(2)}_{\beta}+\mathbf{d}-\mathbf{r})} \cdot$$
$$\cdot\, e^{-i\mathbf{p}'\cdot\mathbf{r}} e^{i(\mathbf{p}'-\mathbf{k})\cdot(\mathbf{R}^{(1)}+\boldsymbol{\tau}^{(1)}_{\alpha})} \tag{5.12}$$

and recognizing the two delta functions when summing over $\mathbf{r}, \mathbf{R}^{(1)}$, we arrive to

$$T^{\alpha,\beta}_{\mathbf{k},\mathbf{p}'} = \sum_{\mathbf{G}^{(1)},\mathbf{G}^{(2)}} \frac{t_{\mathbf{G}^{(2)}+\mathbf{p}'}}{\Omega} \quad \delta(\mathbf{G}^{(1)} + \mathbf{k}, \mathbf{G}^{(2)} + \mathbf{p}') \quad e^{i\mathbf{G}^{(2)}\cdot(\boldsymbol{\tau}^{(2)}_{\beta}+\mathbf{d})-i\mathbf{G}^{(1)}\cdot\boldsymbol{\tau}^{(1)}_{\alpha}} \tag{5.13}$$

where Ω is the area of the graphene unit cell.

Now as shown in [5] the hopping $t_{\mathbf{k}}$ decays exponentially for momenta far from the Dirac point of the graphene Brillouin Zone, i.e. $\mathbf{K}^{(1)}_D = -(\mathbf{b}^{(1)}_1 + \mathbf{b}^{(1)}_2)/3$ and $\mathbf{K}^{(2)}_D = -(\mathbf{b}^{(2)}_1 + \mathbf{b}^{(2)}_2)/3$, so a good approximation is to consider only the leading nearest hopping term, evaluated at the Dirac point, $t_{\mathbf{G}^{(1)}+\mathbf{k}}$, with $|\mathbf{G}^{(1)} + \mathbf{k}| \simeq |\mathbf{K}^{(1)}_D|$, so $t_{\mathbf{G}^{(1)}+\mathbf{k}} \simeq t_{\mathbf{K}^{(1)}_D}$. This is related to the fact that the

separation of the two layers $\mathbf{d}$ exceeds the separation of the carbon atom of more than a factor 2 and this is relevant in the two centers integral for computing $t(r)$.

To understand which the leading terms in equation (5.13) are, we introduce three vectors, as can be seen in figure 5.3 , and this constitutes the edges of the first Moiré Brillouin Zone, i.e. the Brillouin Zone of the superlattice, and they are related to the possible momentum transfer for the hopping term. In particular defining

$$\begin{aligned}\mathbf{q}_1 &= \mathbf{K}_D^{(2)} - \mathbf{K}_D^{(1)} \\ \mathbf{q}_2 &= \mathbf{K}_D^{(2)} + \mathbf{b}_1^{(2)} - \mathbf{K}_D^{(1)} - \mathbf{b}_1^{(1)} \\ \mathbf{q}_3 &= \mathbf{K}_D^{(2)} + \mathbf{b}_2^{(2)} - \mathbf{K}_D^{(1)} - \mathbf{b}_2^{(1)}\end{aligned} \tag{5.14}$$

and remembering that $\mathbf{K}_D^{(l)} = -(\mathbf{b}_1^{(l)} + \mathbf{b}_2^{(l)})/3$

$$\mathbf{K}_D^{(l)} = \frac{4\pi}{3\sqrt{3}a_0} R_{\theta/2}^{(l)} \begin{pmatrix}1\\0\end{pmatrix} \tag{5.15}$$

we can write the components of $\mathbf{q}_j$ using Eq. (5.14)

$$\begin{aligned}
\mathbf{q}_1 &= \frac{4\pi}{3\sqrt{3}a_0} R_{\theta/2}^{(2)} \begin{pmatrix}1\\0\end{pmatrix} - \frac{4\pi}{3\sqrt{3}a_0} R_{\theta/2}^{(1)} \begin{pmatrix}1\\0\end{pmatrix} = \frac{4\pi}{3\sqrt{3}a_0} \left[\begin{pmatrix}\cos(\theta/2)\\ -\sin(\theta/2)\end{pmatrix} - \begin{pmatrix}\cos(\theta/2)\\ \sin(\theta/2)\end{pmatrix} \right] = \\
&= k_\theta \begin{pmatrix}0\\-1\end{pmatrix} \\
\mathbf{q}_2 &= k_\theta \begin{pmatrix}0\\-1\end{pmatrix} + \frac{2\pi}{3a_0} R_{\theta/2}^{(2)} \begin{pmatrix}-\sqrt{3}\\1\end{pmatrix} - \frac{2\pi}{3a_0} R_{\theta/2}^{(1)} \begin{pmatrix}-\sqrt{3}\\1\end{pmatrix} = \\
&= k_\theta \begin{pmatrix}0\\-1\end{pmatrix} + \frac{2\pi}{3a_0} \left[\begin{pmatrix}-\sqrt{3}\cos(\theta/2) + \sin(\theta/2)\\ \sqrt{3}\sin(\theta/2) + \cos(\theta/2)\end{pmatrix} - \begin{pmatrix}-\sqrt{3}\cos(\theta/2) - \sin(\theta/2)\\ -\sqrt{3}\sin(\theta/2) + \cos(\theta/2)\end{pmatrix} \right] = \\
&= k_\theta \begin{pmatrix}0\\-1\end{pmatrix} + k_\theta \begin{pmatrix}\frac{\sqrt{3}}{2}\\ \frac{3}{2}\end{pmatrix} = k_\theta \begin{pmatrix}\frac{\sqrt{3}}{2}\\ \frac{1}{2}\end{pmatrix} \\
\mathbf{q}_3 &= k_\theta \begin{pmatrix}0\\-1\end{pmatrix} + \frac{2\pi}{3a_0} R_{\theta/2}^{(2)} \begin{pmatrix}-\sqrt{3}\\-1\end{pmatrix} - \frac{2\pi}{3a_0} R_{\theta/2}^{(1)} \begin{pmatrix}-\sqrt{3}\\-1\end{pmatrix} = \\
&= k_\theta \begin{pmatrix}0\\-1\end{pmatrix} + \frac{2\pi}{3a_0} \left[\begin{pmatrix}-\sqrt{3}\cos(\theta/2) - \sin(\theta/2)\\ \sqrt{3}\sin(\theta/2) - \cos(\theta/2)\end{pmatrix} - \begin{pmatrix}-\sqrt{3}\cos(\theta/2) + \sin(\theta/2)\\ -\sqrt{3}\sin(\theta/2) - \cos(\theta/2)\end{pmatrix} \right] = \\
&= k_\theta \begin{pmatrix}0\\-1\end{pmatrix} + k_\theta \begin{pmatrix}-\frac{\sqrt{3}}{2}\\ \frac{3}{2}\end{pmatrix} = k_\theta \begin{pmatrix}-\frac{\sqrt{3}}{2}\\ \frac{1}{2}\end{pmatrix}
\end{aligned} \tag{5.16}$$

where $k_\theta = |\mathbf{q}_j| = (8\pi/3\sqrt{3}a_0)\sin(\theta/2)$. The above approximation it is translated to the fact that an electron state with momentum $\mathbf{p}'$ in the second

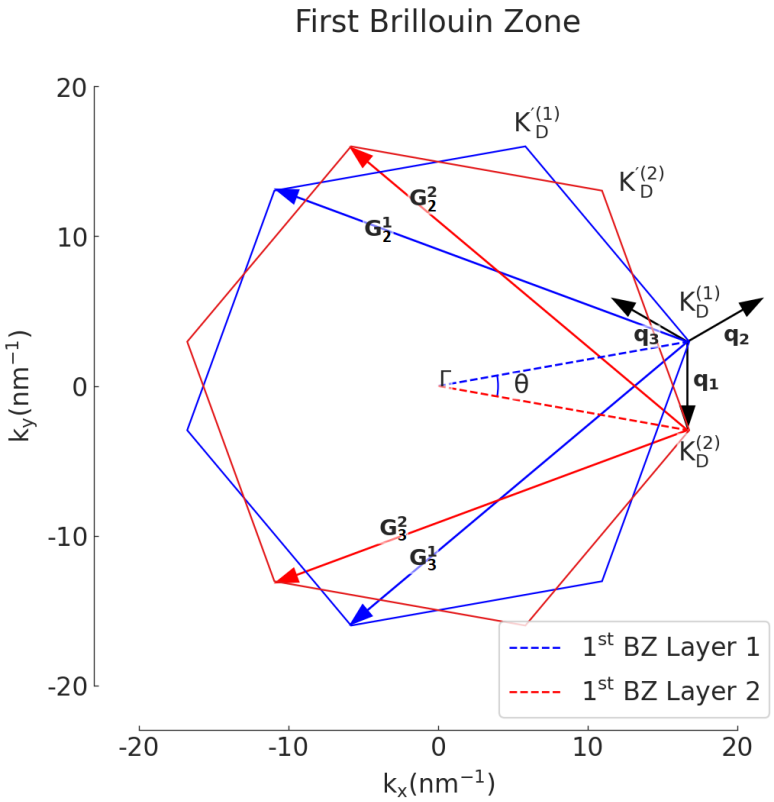

Figure 5.3: $\mathbf{q_i}$ and $\mathbf{G_i^{(1/2)}}$, $i = 1, 2, 3$ vectors

layer can hop to an electron state with momentum $\mathbf{k}$ in the first layer only if $\mathbf{p}' - \mathbf{k} = \mathbf{q}_j$. Under this assumption we can rewrite the tunneling term considering only the three main contributions, where the only $\mathbf{G}^{(1/2)}$ remaining are only the reciprocal lattice vectors which connect the Dirac points to theirs equivalent counterpart is shown in figure (5.3), so $\mathbf{G}_j^{(l)} = m_j \mathbf{b}_1^{(l)} + n_j \mathbf{b}_2^{(l)}$, with $j = 1, 2, 3$, and $(m_1, n_1) = (0, 0)$, $(m_2, n_2) = (1, 0)$, $(m_3, n_3) = (0, 1)$. This, by using the definition of the $\mathbf{q}_j$, leads to

$$T^{\alpha,\beta}(\mathbf{r}) = \omega \sum_{j=1}^{3} e^{-i\mathbf{q}_j \cdot \mathbf{r}} T_j^{\alpha,\beta} \tag{5.17}$$

where $\omega = t_{\mathbf{K}_D}/\Omega$. We underline again that this sum is reduced to only the first MBZ, and so contain only the first three main terms. In the following section, when we will look at the band structure, and we will keep more terms going further in the truncation, but for the study of the low energy limit we

can use only the previous terms from the expansion of the hopping term. To obtain the explicit form for the $T_j^{\alpha,\beta}$ we have to use equation (5.13), and this give us

$$\begin{aligned}
T_1 &= e^{i\mathbf{G}_1^{(2)}\cdot\mathbf{d}}\begin{pmatrix} e^{i\mathbf{G}_1^{(2)}\cdot\boldsymbol{\tau}_A^{(2)}-i\mathbf{G}_1^{(1)}\cdot\boldsymbol{\tau}_A^{(1)}} & e^{i\mathbf{G}_1^{(2)}\cdot\boldsymbol{\tau}_B^{(2)}-i\mathbf{G}_1^{(1)}\cdot\boldsymbol{\tau}_A^{(1)}} \\ e^{i\mathbf{G}_1^{(2)}\cdot\boldsymbol{\tau}_A^{(2)}-i\mathbf{G}_1^{(1)}\cdot\boldsymbol{\tau}_B^{(1)}} & e^{i\mathbf{G}_1^{(2)}\cdot\boldsymbol{\tau}_B^{(2)}-i\mathbf{G}_1^{(1)}\cdot\boldsymbol{\tau}_B^{(1)}} \end{pmatrix} \rightarrow \mathbf{G}_1^{(l)} = 0\mathbf{b}_1^{(l)} + 0\mathbf{b}_2^{(l)} \\
&= e^{i\mathbf{G}_1^{(2)}\cdot\mathbf{d}}\begin{pmatrix} e^0 & e^0 \\ e^0 & e^0 \end{pmatrix} = \begin{pmatrix} 1 & 1 \\ 1 & 1 \end{pmatrix} \\
T_2 &= e^{i\mathbf{G}_2^{(2)}\cdot\mathbf{d}}\begin{pmatrix} e^{i\mathbf{G}_2^{(2)}\cdot\boldsymbol{\tau}_A^{(2)}-i\mathbf{G}_2^{(1)}\cdot\boldsymbol{\tau}_A^{(1)}} & e^{i\mathbf{G}_2^{(2)}\cdot\boldsymbol{\tau}_B^{(2)}-i\mathbf{G}_2^{(1)}\cdot\boldsymbol{\tau}_A^{(1)}} \\ e^{i\mathbf{G}_2^{(2)}\cdot\boldsymbol{\tau}_A^{(2)}-i\mathbf{G}_2^{(1)}\cdot\boldsymbol{\tau}_B^{(1)}} & e^{i\mathbf{G}_2^{(2)}\cdot\boldsymbol{\tau}_B^{(2)}-i\mathbf{G}_2^{(1)}\cdot\boldsymbol{\tau}_B^{(1)}} \end{pmatrix} \rightarrow \mathbf{G}_2^{(l)} = 1\mathbf{b}_1^{(l)} + 0\mathbf{b}_2^{(l)} \\
&= e^{i\mathbf{G}_2^{(2)}\cdot\mathbf{d}}\begin{pmatrix} e^{i\phi} & 1 \\ e^{-i\phi} & e^{i\phi} \end{pmatrix} \\
T_3 &= e^{i\mathbf{G}_3^{(2)}\cdot\mathbf{d}}\begin{pmatrix} e^{i\mathbf{G}_3^{(2)}\cdot\boldsymbol{\tau}_A^{(2)}-i\mathbf{G}_3^{(1)}\cdot\boldsymbol{\tau}_A^{(1)}} & e^{i\mathbf{G}_3^{(2)}\cdot\boldsymbol{\tau}_B^{(2)}-i\mathbf{G}_3^{(1)}\cdot\boldsymbol{\tau}_A^{(1)}} \\ e^{i\mathbf{G}_3^{(2)}\cdot\boldsymbol{\tau}_A^{(2)}-i\mathbf{G}_3^{(1)}\cdot\boldsymbol{\tau}_B^{(1)}} & e^{i\mathbf{G}_3^{(2)}\cdot\boldsymbol{\tau}_B^{(2)}-i\mathbf{G}_3^{(1)}\cdot\boldsymbol{\tau}_B^{(1)}} \end{pmatrix} \rightarrow \mathbf{G}_3^{(l)} = 0\mathbf{b}_1^{(l)} + 1\mathbf{b}_2^{(l)} \\
&= e^{i\mathbf{G}_3^{(2)}\cdot\mathbf{d}}\begin{pmatrix} e^{-i\phi} & 1 \\ e^{i\phi} & e^{-i\phi} \end{pmatrix}
\end{aligned} \tag{5.18}$$

where $\phi = 2\pi/3$ and we have to keep in mind that every time we have $\boldsymbol{\tau}_A^{(2)}$ we have to use instead $\boldsymbol{\tau}_B^{(2)}$ because of the stacking AB. With this we can write explicitly the hopping term from layer 1 to layer 2 in 5.17 as follows

$$\begin{aligned}
T_{\mathbf{k},\mathbf{p}'} = \omega\begin{pmatrix} 1 & 1 \\ 1 & 1 \end{pmatrix}\delta_{\mathbf{k}-\mathbf{p}',-\mathbf{q}_1} + \omega e^{i\mathbf{G}_2^{(2)}\cdot\mathbf{d}}\begin{pmatrix} e^{i\phi} & 1 \\ e^{-i\phi} & e^{i\phi} \end{pmatrix}\delta_{\mathbf{k}-\mathbf{p}',-\mathbf{q}_2} + \\
+ \omega e^{i\mathbf{G}_3^{(2)}\cdot\mathbf{d}}\begin{pmatrix} e^{-i\phi} & 1 \\ e^{i\phi} & e^{-i\phi} \end{pmatrix}\delta_{\mathbf{k}-\mathbf{p}',-\mathbf{q}_3}
\end{aligned} \tag{5.19}$$

and, for accounting instead the hopping from layer 2 to layer 1, one has only to take the adjoint.

Now that we have written the explicit expression of the hopping terms, we can take the limit of $\theta \to 0$ and $\mathbf{d} \to 0$ and verify that in this way our description returns to the one saw in section Double Layer Graphene, i.e. to the AB stacking bilayer description. So

$$\lim_{\substack{\theta\to 0\\ \mathbf{d}\to 0}} T_{\mathbf{k},\mathbf{p}'} = \begin{pmatrix} 1 & 1 \\ 1 & 1 \end{pmatrix} + \omega\begin{pmatrix} e^{i\phi} & 1 \\ e^{-i\phi} & e^{i\phi} \end{pmatrix} + \omega\begin{pmatrix} e^{-i\phi} & 1 \\ e^{i\phi} & e^{-i\phi} \end{pmatrix} = 3\omega\begin{pmatrix} 0 & 1 \\ 0 & 0 \end{pmatrix} \tag{5.20}$$

obtaining again the same form seen before

$$H = \begin{pmatrix} h_1 & T \\ T^\dagger & h_2 \end{pmatrix} = \begin{pmatrix} 0 & t\Delta_{\mathbf{k}} & 0 & t_\perp \\ t\Delta_{\mathbf{k}}^* & 0 & 0 & 0 \\ 0 & 0 & 0 & t\Delta_{\mathbf{k}} \\ t_\perp & 0 & t\Delta_{\mathbf{k}}^* & 0 \end{pmatrix} \tag{5.21}$$

where $h_{1/2}$ stand for the single layer hamiltonian for layer 1/2. This hamiltonian has the same form as long as we consider $t_\perp = 3\omega$. So this give us also the relation between the hopping coefficients of BLG and tBLG.

Now going back to our description, since we are near the Dirac point, we will measure momenta from the Dirac point K (or K' since they are related by symmetry), and the single layer effective hamiltonian, as seen in chapter 1, can be written in the form of $h^K(\mathbf{k}) = \hbar v(k_x\sigma_x - k_y\sigma_y) = \hbar v\boldsymbol{\sigma}^* \cdot \mathbf{k}$ near K point, $h^{K'}(\mathbf{k}) = \hbar v(k_x\sigma_x - k_y\sigma_y) = \hbar v\boldsymbol{\sigma}\cdot\mathbf{k}$ near K' point. By limiting ourselves to the first honeycomb shell, we can write the total hamiltonian as

$$\mathscr{H}^{K,K'_M} = \begin{pmatrix} h^K_{\theta/2}(\mathbf{k}) & wT_1 & wT_2 & wT_3 \\ wT_1^\dagger & h^K_{-\theta/2}(\mathbf{k}-\mathbf{q}_1) & 0 & 0 \\ wT_2^\dagger & 0 & h^K_{-\theta/2}(\mathbf{k}-\mathbf{q}_2) & 0 \\ wT_3^\dagger & 0 & 0 & h^K_{-\theta/2}(\mathbf{k}-\mathbf{q}_3) \end{pmatrix} \tag{5.22}$$

where K'_M is the Dirac point in the superlattice reciprocal space, which corresponds by symmetry to the K point in the graphene reciprocal lattice. In this notation $\mathbf{k}$ is in the Moiré Brillouin Zone, so measured from the Dirac points. This hamiltonian acts on four two-components spinors $\Psi = (\psi_0, \psi_1, \psi_2, \psi_3)$, ψ_0 is at momentum $\mathbf{k}$ near the Dirac point in one layer and the other three ψ_j are at momenta near $\mathbf{q}_j$ in the other layer. To simplify the calculations, since $h^K_{\theta/2}(\mathbf{k})$ depends little on θ which is supposed to be small (as shown by numerical simulations in [5]), we can neglect this dependence, and we will use this simplification in the following sections.

5.3 Low energy limit

We are now interested in calculating the low energy limit, so by focusing on the description near the Dirac points. If we consider the case $\mathbf{k} = 0$, so exactly at the Dirac point, we expect zero energy eigenstate, and this condition becames

$$\mathscr{H}^{K,K'_M}_{(0)}\Psi^{(0)} = 0\Psi^{(0)} \tag{5.23}$$

and this leads to the conditions on the spinor components

$$\begin{cases} h^K(\mathbf{k})\psi_0^{(0)} + wT_1\psi_1^{(0)} + wT_2\psi_2^{(0)} + wT_3\psi_3^{(0)} = 0 \\ h^K(\mathbf{k}-\mathbf{q}_1)\psi_1^{(0)} + wT_1^\dagger\psi_0^{(0)} = 0 \\ h^K(\mathbf{k}-\mathbf{q}_2)\psi_2^{(0)} + wT_2^\dagger\psi_0^{(0)} = 0 \\ h^K(\mathbf{k}-\mathbf{q}_3)\psi_3^{(0)} + wT_3^\dagger\psi_0^{(0)} = 0 \end{cases} \tag{5.24}$$

We note that since we are at $\mathbf{k} \approx 0$, $h^K(\mathbf{k}-\mathbf{q}_j) \simeq h^K(-\mathbf{q}_j)$. This lead to the condition that $\psi_j = -wh_j^{-1}T_j^\dagger\psi_0$ $(j = 1, 2, 3)$ and

$$T_j h_j^{-1} T_j^\dagger = 0 \tag{5.25}$$

to prove this we explicit the calculations

$$\begin{aligned}
h_1 &= \hbar v\boldsymbol{\sigma}^* \cdot (-\mathbf{q}_1) = -\hbar v k_\theta \sigma_y \quad \rightarrow \quad h_1^{-1} = -\frac{1}{\hbar v k_\theta}\sigma_y \\
\Rightarrow \quad T_1 h_1^{-1} T_1^\dagger &\propto \begin{pmatrix} 1 & 1 \\ 1 & 1 \end{pmatrix}\begin{pmatrix} 0 & i \\ -i & 0 \end{pmatrix}\begin{pmatrix} 1 & 1 \\ 1 & 1 \end{pmatrix} = 0 \\
h_2 &= \hbar v\boldsymbol{\sigma}^* \cdot (-\mathbf{q}_2) = \hbar v k_\theta \begin{pmatrix} 0 & e^{-i\frac{5}{6}\pi} \\ e^{i\frac{5}{6}\pi} & 0 \end{pmatrix} \quad \rightarrow \quad h_2^{-1} = \frac{1}{\hbar v k_\theta}\begin{pmatrix} 0 & e^{-i\frac{5}{6}\pi} \\ e^{i\frac{5}{6}\pi} & 0 \end{pmatrix} \\
\Rightarrow \quad T_2 h_2^{-1} T_2^\dagger &\propto \begin{pmatrix} 1 & e^{i\phi} \\ e^{-i\phi} & 1 \end{pmatrix}\begin{pmatrix} 0 & e^{-i\frac{5}{6}\pi} \\ e^{i\frac{5}{6}\pi} & 0 \end{pmatrix}\begin{pmatrix} 1 & e^{i\phi} \\ e^{-i\phi} & 1 \end{pmatrix} \propto \\
&\propto \begin{pmatrix} e^{i\frac{3}{2}\pi} + e^{-i\frac{3}{2}\pi} & e^{i\frac{13}{6}\pi} + e^{-i\frac{5}{6}\pi} \\ e^{-i\frac{13}{6}\pi} + e^{i\frac{5}{6}\pi} & e^{i\frac{3}{2}\pi} + e^{-i\frac{3}{2}\pi} \end{pmatrix} = 0 \\
h_3 &= \hbar v\boldsymbol{\sigma}^* \cdot (-\mathbf{q}_3) = \hbar v k_\theta \begin{pmatrix} 0 & e^{-i\frac{\pi}{6}} \\ e^{i\frac{\pi}{6}} & 0 \end{pmatrix} \quad \rightarrow \quad h_3^{-1} = \frac{1}{\hbar v k_\theta}\begin{pmatrix} 0 & e^{-i\frac{\pi}{6}} \\ e^{i\frac{\pi}{6}} & 0 \end{pmatrix} \\
\Rightarrow \quad T_3 h_3^{-1} T_3^\dagger &\propto \begin{pmatrix} 1 & e^{-i\phi} \\ e^{i\phi} & 1 \end{pmatrix}\begin{pmatrix} 0 & e^{-i\frac{\pi}{6}} \\ e^{i\frac{\pi}{6}} & 0 \end{pmatrix}\begin{pmatrix} 1 & e^{-i\phi} \\ e^{i\phi} & 1 \end{pmatrix} \propto \\
&\propto \begin{pmatrix} e^{i\frac{\pi}{2}} + e^{-i\frac{\pi}{2}} & e^{-i\frac{7}{6}\pi} + e^{i\frac{\pi}{6}} \\ e^{i\frac{7}{6}\pi} + e^{-i\frac{\pi}{6}} & e^{i\frac{\pi}{2}} + e^{-i\frac{\pi}{2}} \end{pmatrix} = 0
\end{aligned} \tag{5.26}$$

where $h_j^{-1} = h^{-1}(-\mathbf{q}_j)$. This can be proved also in a more elegant way by recognizing that the T_j matrices can be rewritten as a combination of Pauli matrices

$$T_1 = 1 + \sigma_x,\ T_2 = e^{i\phi}\left(1 - \frac{1}{2}\sigma_x - \frac{\sqrt{3}}{2}\sigma_y\right),\ T_3 = e^{-i\phi}\left(1 - \frac{1}{2}\sigma_x + \frac{\sqrt{3}}{2}\sigma_y\right) \tag{5.27}$$

so using the property of the Pauli matrices we can obtain the same result

$$
\begin{aligned}
T_1 h_1^{-1} T_1^\dagger &\propto (1+\sigma_x)(-\sigma_y)(1+\sigma_x) = -\sigma_y - \sigma_y\sigma_x - \sigma_x\sigma_y - \sigma_x\sigma_y\sigma_x \\
&\downarrow {\scriptstyle \{\sigma_a,\sigma_b\}=2\delta_{a,b}\mathbb{1}} \\
&= -\sigma_y + \sigma_y\sigma_x\sigma_x \\
&\downarrow {\scriptstyle \sigma_x^2=\sigma_y^2=\sigma_z^2=\mathbb{1}} \\
&= \sigma_y - \sigma_y = 0 \\
T_2 h_2^{-1} T_2^\dagger &\propto \left(1 - \frac{1}{2}\sigma_x - \frac{\sqrt{3}}{2}\sigma_y\right)\left(-\frac{\sqrt{3}}{2}\sigma_x + \frac{1}{2}\sigma_y\right)\left(1 - \frac{1}{2}\sigma_x - \frac{\sqrt{3}}{2}\sigma_y\right) = \\
&= \left(-\frac{\sqrt{3}}{2}\sigma_x + \frac{1}{2}\sigma_y + +\frac{\sqrt{3}}{4}\sigma_x\sigma_x - \frac{1}{4}\sigma_x\sigma_y + \frac{3}{4}\sigma_y\sigma_x - \frac{\sqrt{3}}{4}\sigma_y\sigma_y\right)\cdot \\
&\cdot \left(1 - \frac{1}{2}\sigma_x - \frac{\sqrt{3}}{2}\sigma_y\right) = \\
&\downarrow {\scriptstyle \{\sigma_a,\sigma_b\}=2\delta_{a,b}\mathbb{1},\ \sigma_x^2=\sigma_y^2=\sigma_z^2=\mathbb{1}} \\
&= \left(-\frac{\sqrt{3}}{2}\sigma_x + \frac{1}{2}\sigma_y - \sigma_x\sigma_y\right)\left(1 - \frac{1}{2}\sigma_x - \frac{\sqrt{3}}{2}\sigma_y\right) = \\
&= -\frac{\sqrt{3}}{2}\sigma_x + \frac{\sqrt{3}}{4}\sigma_x\sigma_x + \frac{3}{4}\sigma_x\sigma_y + \frac{1}{2}\sigma_y - \frac{1}{4}\sigma_y\sigma_x - \frac{\sqrt{3}}{4}\sigma_y\sigma_y + \\
&- \sigma_x\sigma_y + \frac{1}{2}\sigma_x\sigma_y\sigma_x + \frac{\sqrt{3}}{2}\sigma_x\sigma_y\sigma_y = \\
&\downarrow {\scriptstyle \{\sigma_a,\sigma_b\}=2\delta_{a,b}\mathbb{1},\ \sigma_x^2=\sigma_y^2=\sigma_z^2=\mathbb{1}} \\
&= 0 \\
T_3 h_3^{-1} T_3^\dagger &\propto \left(1 - \frac{1}{2}\sigma_x + \frac{\sqrt{3}}{2}\sigma_y\right)\left(\frac{\sqrt{3}}{2}\sigma_x + \frac{1}{2}\sigma_y\right)\left(1 - \frac{1}{2}\sigma_x + \frac{\sqrt{3}}{2}\sigma_y\right) = \\
&\downarrow {\scriptstyle \{\sigma_a,\sigma_b\}=2\delta_{a,b}\mathbb{1},\ \sigma_x^2=\sigma_y^2=\sigma_z^2=\mathbb{1}} \\
&= \left(\frac{\sqrt{3}}{2}\sigma_x + \frac{1}{2}\sigma_y - \sigma_x\sigma_y\right)\left(1 - \frac{1}{2}\sigma_x + \frac{\sqrt{3}}{2}\sigma_y\right) = \\
&= \frac{\sqrt{3}}{2}\sigma_x - \frac{\sqrt{3}}{4}\sigma_x\sigma_x + \frac{3}{4}\sigma_x\sigma_y + \frac{1}{2}\sigma_y - \frac{1}{4}\sigma_y\sigma_x - \sigma_x\sigma_y + \\
&+ \frac{1}{2}\sigma_x\sigma_y\sigma_x - \frac{\sqrt{3}}{2}\sigma_x\sigma_y\sigma_y = \\
&\downarrow {\scriptstyle \{\sigma_a,\sigma_b\}=2\delta_{a,b}\mathbb{1},\ \sigma_x^2=\sigma_y^2=\sigma_z^2=\mathbb{1}} \\
&= 0
\end{aligned}
\tag{5.28}
$$

This proves also, substituting in the first equation of 5.24, that the equation for ψ_0 is $h_0\psi_0 = 0$, i.e. ψ_0 is one of the two zero energy states of the isolated layer, $\psi_0^{(1)}$ or $\psi_0^{(2)}$.

From this we see that we can express ψ_j as function of ψ_0, so the hamiltonian, using a perturbative approach, can be folded in an effective hamiltonian for the low energy state on the ψ_0 space with $\psi_{j,\mathbf{k}} \approx -wh_j^{-1}T_j^\dagger\psi_{0,\mathbf{k}}$ $(j = 1, 2, 3)$ (these terms comes from the system 5.24):

$$H^{K,K'_M}_{eff,(1)}(\mathbf{k}) = \frac{\langle\Psi|\,\mathscr{H}^{K,K'_M}\,|\Psi\rangle}{\langle\Psi|\Psi\rangle} \tag{5.29}$$

and substituting we have that

$$\begin{aligned}\langle\Psi|\Psi\rangle &= \begin{pmatrix}\psi_0^\dagger & (-wh_1^{-1}T_1^\dagger\psi_0)^\dagger & (-wh_2^{-1}T_2^\dagger\psi_0)^\dagger & (-wh_3^{-1}T_3^\dagger\psi_0)^\dagger\end{pmatrix}\begin{pmatrix}\psi_0\\ -wh_1^{-1}T_1^\dagger\psi_0\\ -wh_2^{-1}T_2^\dagger\psi_0\\ -wh_3^{-1}T_3^\dagger\psi_0\end{pmatrix} = \\ &= ||\psi_0||^2 + w^2\sum_{i=1}^{3}(h_i^{-1}T_i^\dagger\psi_0)^\dagger(-h_i^{-1}T_i^\dagger\psi_0) = \\ &= ||\psi_0||^2 + w^2\sum_{i=1}^{3}\psi_0^\dagger T_i(-h_i^{-1})^\dagger(-h_i^{-1})T_i^\dagger\psi_0\end{aligned} \tag{5.30}$$

we compute $(-h_i^{-1})^\dagger(-h_i^{-1})$ for $i = 1, 2, 3$

$$\begin{aligned}(-h_1^{-1})^\dagger(-h_1^{-1}) &= \frac{1}{(\hbar vk_\theta)^2}\sigma_y^\dagger\sigma_y = \frac{1}{(\hbar vk_\theta)^2}\mathbb{1}\\ (-h_2^{-1})^\dagger(-h_2^{-1}) &= \frac{1}{(\hbar vk_\theta)^2}\left(\frac{\sqrt{3}}{2}\sigma_x - \frac{1}{2}\sigma_y\right)^\dagger\left(\frac{\sqrt{3}}{2}\sigma_x - \frac{1}{2}\sigma_y\right) = \frac{1}{(\hbar vk_\theta)^2}\mathbb{1}\\ (-h_3^{-1})^\dagger(-h_3^{-1}) &= \frac{1}{(\hbar vk_\theta)^2}\left(-\frac{\sqrt{3}}{2}\sigma_x - \frac{1}{2}\sigma_y\right)^\dagger\left(-\frac{\sqrt{3}}{2}\sigma_x - \frac{1}{2}\sigma_y\right) = \frac{1}{(\hbar vk_\theta)^2}\mathbb{1}\end{aligned} \tag{5.31}$$

where we use the hermitianity of the Pauli matrices and $\{\sigma_a, \sigma_b\} = 2\delta_{a,b}\mathbb{1}$. Equation (5.30) becomes

$$\langle\Psi|\Psi\rangle = ||\psi_0||^2 + \left(\frac{w}{\hbar vk_\theta}\right)^2\sum_{i=1}^{3}\psi_0^\dagger T_i T_i^\dagger\psi_0 \tag{5.32}$$

If we consider that the phase factor of T_2, T_3 when multiplied with its adjoint give 1, the T_i are combination of hermitian matrices so they are also hermitian,

and what is left to compute is T_i^2

$$\begin{aligned}
T_1^2 &= (1+\sigma_x)(1+\sigma_x) = 2(1+\sigma_x) \\
T_2^2 &= \left(1-\frac{1}{2}\sigma_x-\frac{\sqrt{3}}{2}\sigma_y\right)\left(1-\frac{1}{2}\sigma_x-\frac{\sqrt{3}}{2}\sigma_y\right) = 2\left(1-\frac{1}{2}\sigma_x-\frac{\sqrt{3}}{2}\sigma_y\right) \\
T_3^2 &= \left(1-\frac{1}{2}\sigma_x+\frac{\sqrt{3}}{2}\sigma_y\right)\left(1-\frac{1}{2}\sigma_x+\frac{\sqrt{3}}{2}\sigma_y\right) = 2\left(1-\frac{1}{2}\sigma_x+\frac{\sqrt{3}}{2}\sigma_y\right)
\end{aligned} \tag{5.33}$$

and finally we have

$$\begin{aligned}
\langle\Psi|\Psi\rangle = ||\psi_0||^2 + \left(\frac{w}{\hbar v k_\theta}\right)^2 2\psi_0^\dagger\left[3\mathbb{1}+\sigma_x-\frac{1}{2}\sigma_x-\frac{\sqrt{3}}{2}\sigma_y-\frac{1}{2}\sigma_x+\frac{\sqrt{3}}{2}\sigma_y\right]\psi_0 = \\
= 1+6\left(\frac{w}{\hbar v k_\theta}\right)^2 = 1+6\alpha^2
\end{aligned} \tag{5.34}$$

where $\alpha = w/(\hbar v k_\theta)$. We can now evaluate $H^{K,K'_M}_{eff,(1)}(\mathbf{k})$

$$\begin{aligned}
&= \frac{1}{1+6\alpha^2}\begin{pmatrix}\psi_0^\dagger & (-wh_1^{-1}T_1^\dagger\psi_0)^\dagger & (-wh_2^{-1}T_2^\dagger\psi_0)^\dagger & (-wh_3^{-1}T_3^\dagger\psi_0)^\dagger\end{pmatrix}\mathscr{H}\begin{pmatrix}\psi_0\\ -wh_1^{-1}T_1^\dagger\psi_0\\ -wh_2^{-1}T_2^\dagger\psi_0\\ -wh_3^{-1}T_3^\dagger\psi_0\end{pmatrix} = \\
&= \frac{1}{1+6\alpha^2}\Bigg[\psi_0^\dagger h(\mathbf{k})\psi_0 - w^2\psi_0^\dagger\underbrace{\sum_{i=1}^3 T_i h_i^{-1}T_i^\dagger}_{(1)}\psi_0 + w^2\underbrace{\sum_{i=1}^3\psi_0^\dagger T_i(-h_i^{-1})^\dagger T_i^\dagger\psi_0}_{(2)} + \\
&\qquad + w^2\underbrace{\sum_{i=1}^3\psi_0^\dagger T_i(-h_i^{-1})^\dagger(-h(\mathbf{k}-\mathbf{q}_i)h_i^{-1}T_i^\dagger\psi_0)}_{(3)}\Bigg]
\end{aligned} \tag{5.35}$$

where we omitted the indices K, K'_M to simplify the notation. The summations (1) and (2), using the hermitianity of the matrices and remembering

equation (5.25), are equal to 0, leaving only

$$
\begin{aligned}
H^{K,K'_M}_{eff,(1)}(\mathbf{k}) &= \frac{1}{1+6\alpha^2}\left[\psi_0^\dagger h(\mathbf{k})\psi_0 + w^2\sum_{i=1}^{3}\psi_0^\dagger T_i(h_i^{-1})^\dagger[h(\mathbf{k}-\mathbf{q}_i)h_i^{-1}T_i^\dagger]\psi_0\right] = \\
&\downarrow {\scriptstyle h(\mathbf{k}-\mathbf{q}_i)=h(\mathbf{k})-h_i} \\
&= \frac{1}{1+6\alpha^2}\left\{\psi_0^\dagger h(\mathbf{k})\psi_0 + w^2\sum_{i=1}^{3}\psi_0^\dagger\left[\left(T_i(h_i^{-1})^\dagger h(\mathbf{k})h_i^{-1}T_i^\dagger\right)+\right.\right. \\
&\qquad \left.\left.\underbrace{-\left(T_i(h_i^{-1})^\dagger \underbrace{h_i h_i^{-1}}_{\mathbb{1}} T_i^\dagger\right)}_{0}\right]\psi_0\right\} = \\
&= \frac{\hbar v}{1+6\alpha^2}\psi_0^\dagger\left[\boldsymbol{\sigma}^*\cdot\mathbf{k} + w^2\sum_{i=1}^{3}T_i(h_i^{-1})^\dagger\boldsymbol{\sigma}^*\cdot\mathbf{k}h_i^{-1}T_i^\dagger\right]\psi_0
\end{aligned}
\tag{5.36}
$$

we evaluate separately the three contributions of the summation

$$
\begin{aligned}
T_1(h_1^{-1})^\dagger\boldsymbol{\sigma}^*\cdot\mathbf{k}h_1^{-1}T_1^\dagger &= \frac{1}{(\hbar v k_\theta)^2}(-\sigma_y-\sigma_y\sigma_x)(k_x\sigma_x-k_y\sigma_y)(-\sigma_y+\sigma_y\sigma_x) = \\
&= -2(1+\sigma_x)k_x
\end{aligned}
$$

$$
\begin{aligned}
T_2(h_2^{-1})^\dagger\boldsymbol{\sigma}^*\cdot\mathbf{k}h_2^{-1}T_2^\dagger &= \frac{1}{(\hbar v k_\theta)^2}\left(\sigma_y\sigma_x-\frac{\sqrt{3}}{2}\sigma_x+\frac{1}{2}\sigma_y\right)\left(k_x\sigma_x-k_y\sigma_y\right)\cdot \\
&\quad\cdot\left(-\sigma_y\sigma_x-\frac{\sqrt{3}}{2}\sigma_x+\frac{1}{2}\sigma_y\right) = \\
&= \frac{1}{(\hbar v k_\theta)^2}\left[-\frac{1}{2}\sigma_x k_x+\frac{3}{2}\sigma_y k_y+\frac{\sqrt{3}}{2}\sigma_x k_y+\right. \\
&\qquad\left.-\frac{\sqrt{3}}{2}\sigma_y k_x+k_x-\sqrt{3}k_y\right]
\end{aligned}
$$

$$T_3(h_3^{-1})^\dagger \boldsymbol{\sigma^*}\cdot\mathbf{k}h_3^{-1}T_3^\dagger = \frac{1}{(\hbar v k_\theta)^2}\left(\sigma_y\sigma_x + \frac{\sqrt{3}}{2}\sigma_x + \frac{1}{2}\sigma_y\right)\left(k_x\sigma_x - k_y\sigma_y\right)\cdot$$
$$\cdot\left(-\sigma_y\sigma_x + \frac{\sqrt{3}}{2}\sigma_x + \frac{1}{2}\sigma_y\right) =$$
$$= \frac{1}{(\hbar v k_\theta)^2}\left[-\frac{1}{2}\sigma_x k_x + \frac{\sqrt{3}}{2}\sigma_y k_x + \frac{3}{2}\sigma_y k_y + \right.$$
$$\left. - \frac{\sqrt{3}}{2}\sigma_x h_y + \sqrt{3}k_y + k_x\right] \tag{5.37}$$

and summing this terms all together we obtain

$$H^{K,K'_M}_{eff,(1)}(\mathbf{k}) = \frac{\hbar v}{1+6\alpha^2}\psi_0^\dagger\left[\boldsymbol{\sigma^*}\cdot\mathbf{k} - 3\alpha^2\boldsymbol{\sigma^*}\cdot\mathbf{k}\right]\psi_0 = \hbar v\frac{1-3\alpha^2}{1+6\alpha^2}\psi_0^\dagger\boldsymbol{\sigma^*}\cdot\mathbf{k}\psi_0 =$$
$$= \hbar v^*\psi_0^\dagger\boldsymbol{\sigma^*}\cdot\mathbf{k}\psi_0 \tag{5.38}$$

with $v^* = v\frac{1-3\alpha^2}{1+6\alpha^2}$. So we can notice that the system has the same hamiltonian of the monolayer graphene but with a rescaled Fermi velocity.

It is important to remember that the hamiltonian in (5.38) is characterized by the K, K'_M labels. This means that the hamiltonian is calculated in the proximity of the K point of layer 1 and in the corresponding K'_M point in the Moiré Brillouin zone. In general considering the symmetries of our problem, we have in total eight Dirac fermions labeled by the graphene monolayer valleys, K and K', Moiré valleys, K_M and K'_M, and spins, $\uparrow$ and $\downarrow$ indices. So in general a state of the system must be labeled by three indices that we will call $\eta = \pm 1$ for the valley, $\xi = \pm 1$ for the Moiré valley and $s = \pm 1$ for the spin.

5.4 Results

In general to inspect the band structure of tBLG we cannot use the simplification of equation (5.22) because, as said previously, that was the Hamiltonian after a truncation to the first Moiré Brillouin zone (MBZ), retaining only the main contributions. For our aim one has to consider higher terms, i.e. truncating the hamiltonian after retaining contributions coming from successive Brillouin zones, using the reciprocal Moiré lattice vectors. If we call the Moiré reciprocal lattice vectors as $\mathbf{b}_1^M, \mathbf{b}_2^M$ the general transferred momenta allowed, that in equation (5.14) was written only for the first MBZ, can be written as

$$\begin{aligned} \mathbf{q}_1 &= \mathbf{K}_D^{(2)} - \mathbf{K}_D^{(1)} \\ \mathbf{q}_2 &= \mathbf{K}_D^{(2)} - \mathbf{K}_D^{(1)} + \mathbf{b}_2^M \\ \mathbf{q}_3 &= \mathbf{K}_D^{(2)} - \mathbf{K}_D^{(1)} + \mathbf{b}_1^M \end{aligned} \tag{5.39}$$

For this reason we write a generic state of the system in the Moiré Brillouin zone as

$$|\psi_{\mathbf{k}}^M\rangle = \sum_{l,\alpha,m_1,m_2} u_\alpha^{(l)} \, |l, \alpha, \mathbf{k}, (m_1, m_2)\rangle \tag{5.40}$$

where we introduce the basis

$$|l, \alpha, \mathbf{k}, (m_1, m_2)\rangle = |l, \mathbf{K}^{(l)} + \mathbf{k} + m_1\mathbf{b}_1^M + m_2\mathbf{b}_2^M, \alpha\rangle \, .$$

Let us generalize eq. (5.22): by truncating the basis after retaining higher orders, one can refine the previous result. To be more precise we can show the form of the matrix if we take, for example, a basis in which also other contributions are retained:

$$|1,0,0\rangle\,, |2,0,0\rangle\,, |2,0,1\rangle\,, |2,-1,0\rangle\,, |1,0,-1\rangle\,, |1,1,0\rangle\,, |1,0,1\rangle\,, |1,1,1\rangle\,, |1,-1,0\rangle\,, |1,-1,-1\rangle$$

where we drop for simplicity the sublattice index and the momentum. With the choice of this basis the tight binding hamiltonian becomes

$$\mathscr{H}^{K,K'_M} = \begin{pmatrix} h_1^K & \omega T_1 & \omega T_2 & \omega T_3 & 0 & 0 & 0 & 0 & 0 & 0 \\ \omega T_1^\dagger & h_2^K & 0 & 0 & \omega T_2^\dagger & \omega T_3^\dagger & 0 & 0 & 0 & 0 \\ \omega T_2^\dagger & 0 & h_2^K & 0 & 0 & 0 & \omega T_1^\dagger & \omega T_3^\dagger & 0 & 0 \\ \omega T_3^\dagger & 0 & 0 & h_2^K & 0 & 0 & 0 & 0 & \omega T_1^\dagger & \omega T_2^\dagger \\ 0 & \omega T_2 & 0 & 0 & h_1^K & 0 & 0 & 0 & 0 & 0 \\ 0 & \omega T_3 & 0 & 0 & 0 & h_1^K & 0 & 0 & 0 & 0 \\ 0 & 0 & \omega T_1 & 0 & 0 & 0 & h_1^K & 0 & 0 & 0 \\ 0 & 0 & \omega T_3 & 0 & 0 & 0 & 0 & h_1^K & 0 & 0 \\ 0 & 0 & 0 & \omega T_1 & 0 & 0 & 0 & 0 & h_1^K & 0 \\ 0 & 0 & 0 & \omega T_2 & 0 & 0 & 0 & 0 & 0 & h_1^K \end{pmatrix} \tag{5.41}$$

where $h_1^K = h_1^K(\mathbf{k} + m_1\mathbf{b}_1^M + m_2\mathbf{b}_2^M)$ single layer hamiltonian of layer 1, and $h_2^K = h_2^K(\mathbf{k} + \mathbf{q}_1 + m_1\mathbf{b}_1^M + m_2\mathbf{b}_2^M)$ single layer hamiltonian of layer 2. So by computing the eigenvalues of the previous hamiltonian, one obtains an approximation for the tBLG band structure, which can be improved by considering more and more reciprocal lattice vectors.

5.4.1 Study on the truncation

In this section we study how the calculation for the energy bands depends on the truncation of the general Hamiltonian. An accurate this calculation either for the energy bands and for the density of states is important also when we will consider the interacting case for a reasonable estimate of the superconducting critical temperature that we will do in the last section. We, therefore, solve numerically the eigenvalue problem for an increasing value of the cut, i.e. a higher cut keeps more Moiré Brillouin zones (MBZ) in consideration, so the dimension of the hamiltonian matrix grows as the cut increases. We then calculate the relative error of the obtained results with respect the highest cut we could use, and this value was fixed, due to our available computation power, to a cut at the 8^{th} MBZ. The first consideration we can do is that the relative error depends on the value of the angle considered. The explanation to this lies in the band structure itself: starting from small angles, around the first magic angle, the band are more concentrated around the Fermi energy with respect to the higher angle case. This means that more MBZ are needed to evaluate correctly the correction to the energy. This can be seen in particular comparing the different plots in figure 5.4, in fact although the angle variation is small one can observe that the relative error is much higher for smaller angles [2] $\simeq 10^{-6}$ while riches the computational limit, around $\simeq 10^{-14}$, increasing the value of the angle. The fluctuations that we can see around the relative error $\simeq 10^{-14}$ have not a physical meaning but are numerical fluctuations, because we reach the numerical limit. The estimate of the band energy around the first magic angle ($\theta = 1.05$) reaches the error limit with a truncation to the 6^{th} MBZ, while for $\theta = 5°$ are enough 4 MBZs. We will use a truncation up to the 8^{th} MBZ, to be sure of working with great accuracy for any value of the twist angle. We notice also that the errors are greater in the proximity of the borders of the MBZ, because they are points of high symmetry so more MBZ are needed for the correct evaluation of the energy bands.

[2] The relative error is calculated on a scale between 0 and 1

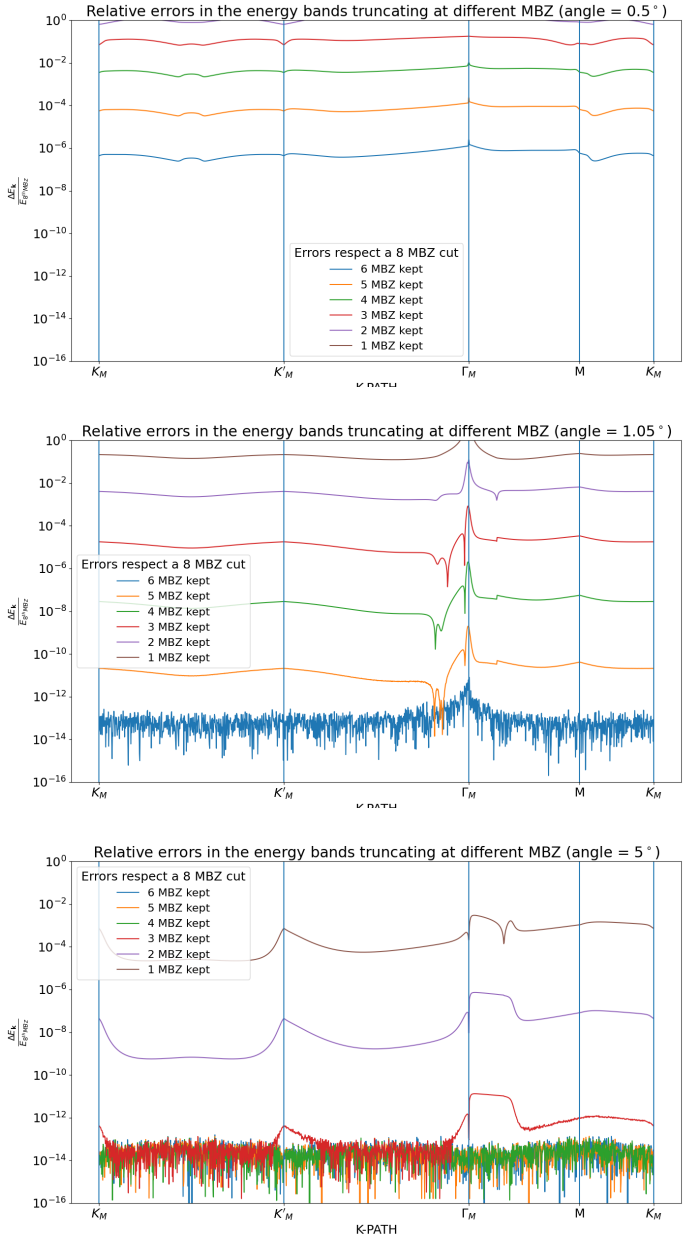

Figure 5.4: Relative errors in the estimation of the energy bands, for different values of the angle (from top to bottom) 0.5°, 1.05°, 5°. The relative errors are calculated with respect to the highest cut we can set (cut up to the 8^{th} Moiré Brillouin Zone)

5.4.2 Band structure

We use an approximation up to the 8th Moiré Brillouin zone and study the differences between the band structure for different values of the twist angle. Since the Moiré BZ is 2D, the band structure is a 3D plot, but to make the comparison easier we choose the path in figure 5.5 to evaluate the band structure. We solve the eigenvalues problem finding the band structure of figure 5.6.

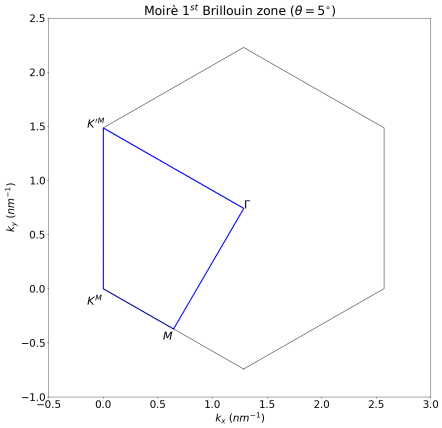

Figure 5.5: K-path in the Moiré BZ used for computing the band structure

From the band structure and density of states we can see how the energies change when we are near and far from the first magic angle. In all the angles studied the bands structure is gapless in proximity of the Dirac points, so the bands meet in the proximity of the Fermi level, and, as we said previously, this is linked to the presence of the massless excitations in proximity of these points.

It is important to underline that in the left plot of Fig. 5.6 the center $(0, 0)$ is one of the Moiré Dirac point. To understand better the picture we highlight in Fig. 5.7 the points of interest and the boundaries of the first Moiré Brillouin zone, so basically we superimpose figure 5.5 on the right pictures of figure 5.6.

Looking at Fig. 5.7 we remember that the zero of our momenta is the first Dirac point $\mathbf{K}^M$.

Although the bands are quite thin also for very small angle, the flat bands only appears in the proximity of the magic angle, and as we move a bit from that, conduction and valence bands become wider and wider, as can be seen

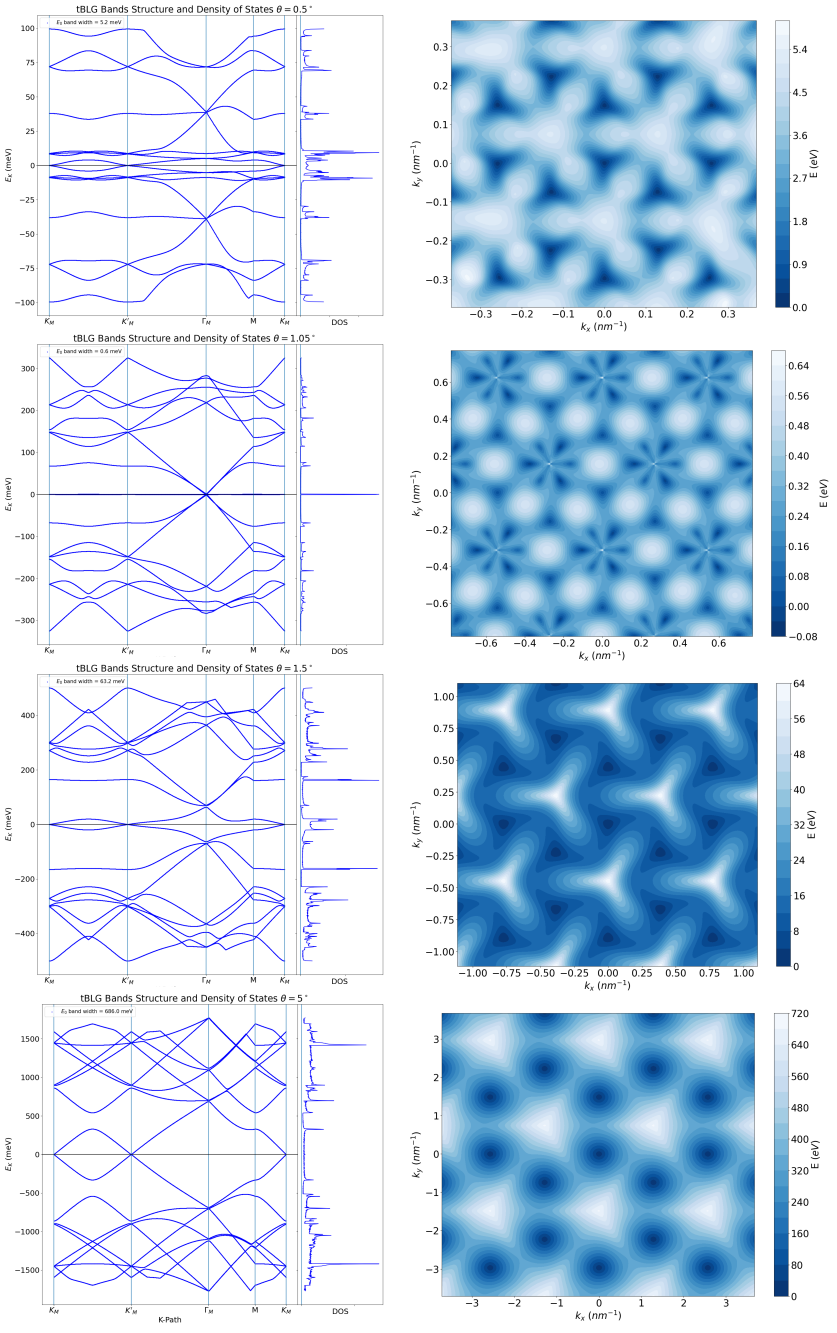

Figure 5.6: tBLG band structure: along the path of fig.5.5 (right), and the first band in 2D (left) for different angles form top to bottom: 0.5°, 1.05°, 1.5°, 5.0°

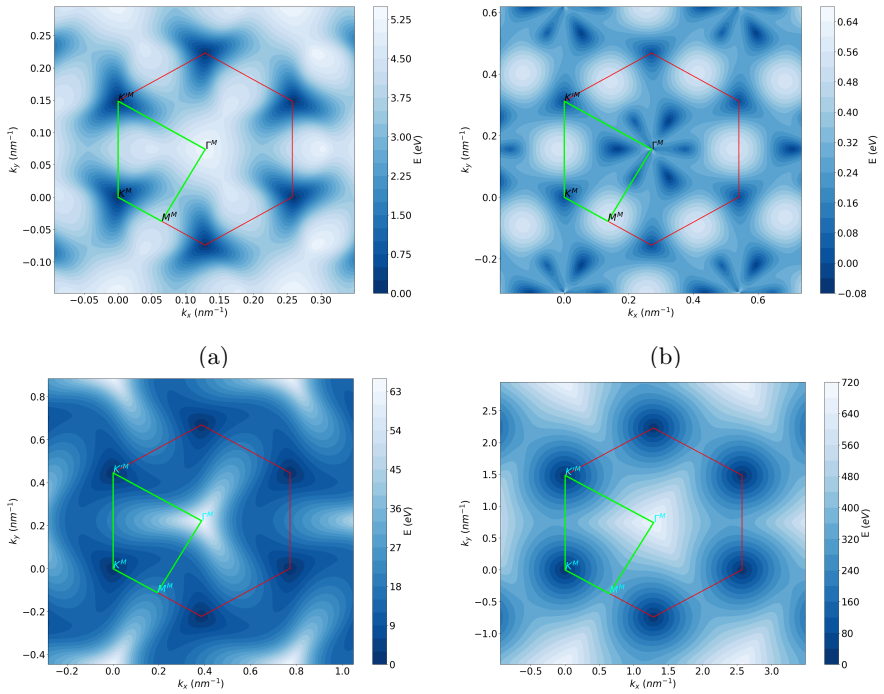

Figure 5.7

comparing figure 5.6 (b) and (c): moving from $\theta \simeq 1.05° \to 1.5°$ the bandwidth increases from 0.6 meV to 64 meV, so a growth of two orders of magnitude. We can notice also how the periodicity is preserved for all the small angles studied, the pattern of maxima and minima does not change, except for the magic angle in which other three minima appears. One can also compute the rescaled Fermi velocity of the system in proximity of the Moiré Dirac point, and this can be done using the same Hamiltonian used for the Moiré bands calculation. This is done by using the general relation between the energy spectrum and the band velocity, i.e.

$$v_{n,\mathbf{K}^M} = \frac{1}{\hbar}\nabla_{\mathbf{k}}\varepsilon_n(\mathbf{k})\big|_{\mathbf{K}^M} \tag{5.42}$$

and since we are interested in the lowest electron state we search for $v_{0,\mathbf{K}^M}$. In particular we are interested in the relation between the rescaled velocity and the parameter α^2, that is the one appearing in the folded hamiltonian (5.38), since the zeros of α^2 are linked to the ones of the rescaled Fermi velocity.

Figure 5.8 on one hand shows us the appearance of the magic angles, the

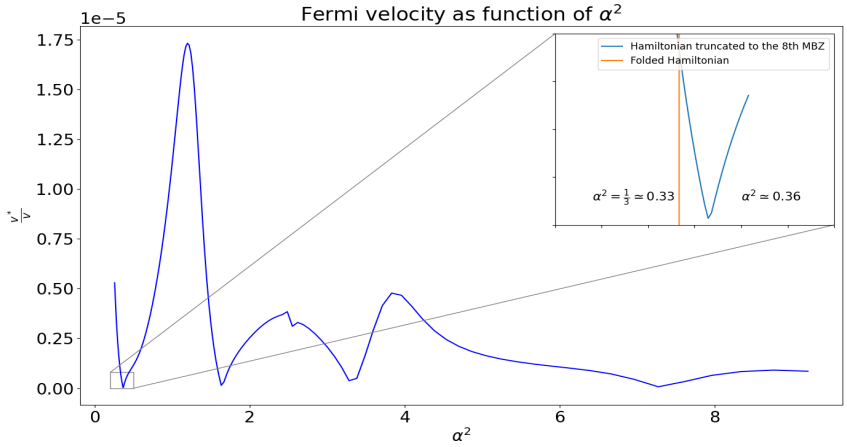

Figure 5.8: Band velocity in proximity of the Dirac point $\mathbf{K}^M$ as function of α^2 (we set for simplicity $\hbar = 1$). The points where the velocity becomes null are called *magic angles*. In the inset we make a comparison with the estimation of the first magic angle using the effective hamiltonian (5.38)

points in which the rescaled Fermi velocity vanishes, and on the other hand gives us an hint on the behavior of the bands as function of the angles. In fact, looking at its definition, the band velocity is linked to the gradient of the energy spectrum, so angles in which the velocity has an high value corresponds to angles in which the bands are wider than the ones with low velocity values.

Instead if one is interested in the low energy property one can use hamiltonian (5.38) and study how the bands look near the Dirac points. In particular this is useful if one is interested in studying what causes the flattening of the band near the first magic angle. So we study how the Dirac velocity v^* depends on the angle in our low energy approximation. Using the explicit form for the Fermi velocity obtained in eq. (5.38), one can clearly see that it vanishes when

$$v^* = \frac{1 - 3\alpha^2}{1 + 6\alpha^2} v = 0 \rightarrow \alpha^2 = \frac{1}{3} \tag{5.43}$$

this corresponds, by expressing it as function of the twisted angle θ, to $\theta = 1.05°$, and this can be computed by remembering the relation $\alpha = w/(\hbar v k_\theta)$. This result predicts with a good accordance with experiments, the first magic angle, as can be seen from fig. 5.8. It is important to notice that the folding of the hamiltonian can be used correctly up to the first magic angle, since we are folding onto the lowest energy band. To describe higher energy bands and higher energy scales one cannot use the hamiltonian (5.38) anymore.

5.5 BCS theory applied to tBLG

We are now interested in studying the superconducting properties of the tBLG. We will use the BCS theory, i.e. we introduce to our model an interaction between fermions which is mediated by the coupling with phonons. We will use for our calculation the folded hamiltonian, since we are interested in the low energy limit, and we will look at the results in the proximity of the magic angle, where the band is quite flat and very near to the Fermi energy. For this purpose we rewrite the Hamiltonian in second quantization, with all the indices

$$H_{tb}^{\eta,\xi,s}(\mathbf{k}) = -\hbar v^* \psi_0^\dagger \boldsymbol{\sigma}^* \cdot \mathbf{k}\psi_0 = -\varepsilon_{\mathbf{k}} c^\dagger_{\mathbf{k},\eta,\xi,s} c_{\mathbf{k},\eta,\xi,s} \tag{5.44}$$

where $\varepsilon_{\mathbf{k}} = \frac{1-3\alpha^2}{1+6\alpha^2}\hbar v\,(\mathbf{k} - k_F)$ are the single-particle energies measured from the Fermi surface and we use $\psi_0^{\eta,\xi,s}(\mathbf{k}) = \phi_0^\eta(\mathbf{k}) c_{\mathbf{k}}^{\eta,\xi,s}$, with $\phi_0^\eta(\mathbf{k})$ the lowest energy eigenfunction of the Hamiltonian.
To proceed with our analysis we have to take into account the electron-phonon interaction.

5.5.1 Phononic hamiltonian

In this section we introduce the bosonic hamiltonian for tBLG. We summarize the general approach to introduce the harmonic model for a crystal. In the introduction to the tight-binding model we introduced the Born-Oppenheimer approximation, and this allow us to decouple the motion of electrons from that of the bosons, and the lattice potential can be seen "frozen", from the point of view of the electrons, because their motion is faster than that of the bosons. But this is true only at first approximation, because if we want to describe the lattice in a proper way we have to consider that lattice sites are the equilibrium positions of the atoms, but they are free to vibrate around these positions. So the first thing to do is to describe the position for an atom at time t as the lattice vector pointing at that site, $\mathbf{R}$, which fixes the equilibrium position inside the lattice, plus a small displacement, that will depend on time and on the considered site

$$\mathbf{r}(\mathbf{R}, t) = \mathbf{R} + \boldsymbol{\delta}\mathbf{u}(\mathbf{R}, t). \tag{5.45}$$

The system of atoms confined on a lattice, can be described by a potential energy U, that is a function of the positions of all the atoms in the crystal, $U(\mathbf{r}_1, ..., \mathbf{r}_N)$ (if we think to a system made of N atoms). The first approximation we introduce to simplify the problem is the pair approximation, i.e. we assume that this potential can be written as a sum over pair interactions, that

depends only on the distance between the two atoms, so we write

$$\begin{aligned} U(\mathbf{r}_1,...,\mathbf{r}_N) &= \frac{1}{2}\sum_{\mathbf{R},\mathbf{R}'}\Phi\left(\mathbf{r}-\mathbf{r}'\right) \\ &\Big\downarrow \text{5.45} \\ &= \frac{1}{2}\sum_{\mathbf{R},\mathbf{R}'}\Phi\Big(\mathbf{R}-\mathbf{R}'+\underbrace{\boldsymbol{\delta}\mathbf{u}(\mathbf{R})-\boldsymbol{\delta}\mathbf{u}'(\mathbf{R}')}_{(1)}\Big). \end{aligned} \tag{5.46}$$

where we hide the dependence on time to simplify the notation. To proceed now we think at the displacement: we said that this displacement represent the vibration of the atom around its equilibrium position, so it is a small deviation from it with respect to the typical size of the lattice, so the lattice constant a. This means that if the we assume true the considerations on $\boldsymbol{\delta}\mathbf{u}(\mathbf{R})$, also (1) must be small, i.e. $|\boldsymbol{\delta}\mathbf{u}(\mathbf{R})-\boldsymbol{\delta}\mathbf{u}'(\mathbf{R}'))| << a$. With this in mind one make a Taylor expansion of the potential energy, truncating it to the harmonic contribution (second order derivatives), obtaining

$$\begin{aligned} U(\mathbf{r}_1,...,\mathbf{r}_N) \simeq \frac{1}{2}\sum_{\mathbf{R},\mathbf{R}'}\Phi\left(\mathbf{R}-\mathbf{R}'\right)+\frac{1}{2}\sum_{\mathbf{R},\mathbf{R}'}\Big(\boldsymbol{\delta}\mathbf{u}(\mathbf{R})-\boldsymbol{\delta}\mathbf{u}(\mathbf{R}')\Big)\nabla\Phi\big|_{\boldsymbol{\delta}\mathbf{u},\boldsymbol{\delta}\mathbf{u}'=0}+ \\ +\frac{1}{4}\sum_{\mathbf{R},\mathbf{R}'}\left[\left(\boldsymbol{\delta}\mathbf{u}(\mathbf{R})-\boldsymbol{\delta}\mathbf{u}(\mathbf{R}')\right)\cdot\nabla\right]^2\Phi\big|_{\boldsymbol{\delta}\mathbf{u},\boldsymbol{\delta}\mathbf{u}'=0} \end{aligned} \tag{5.47}$$

where for simplicity we hide the dependence on the $\Phi\big(\mathbf{R}-\mathbf{R}'+\boldsymbol{\delta}\mathbf{u}(\mathbf{R})-\boldsymbol{\delta}\mathbf{u}'(\mathbf{R}')\big)$ term, and we call $\boldsymbol{\delta}\mathbf{u}(\mathbf{R}')=\boldsymbol{\delta}\mathbf{u}'$. Now focusing on the second term of eq, 5.47, we can rewrite it as:

$$\begin{aligned} &\frac{1}{2}\sum_{\mathbf{R},\mathbf{R}'}\boldsymbol{\delta}\mathbf{u}(\mathbf{R})-\boldsymbol{\delta}\mathbf{u}(\mathbf{R}')\nabla\Phi\big|_{\boldsymbol{\delta}\mathbf{u},\boldsymbol{\delta}\mathbf{u}'=0}= \\ &=\frac{1}{2}\sum_{\mathbf{R}}\boldsymbol{\delta}\mathbf{u}(\mathbf{R})\underbrace{\sum_{\mathbf{R}'}\nabla\Phi\big|_{\boldsymbol{\delta}\mathbf{u},\boldsymbol{\delta}\mathbf{u}'=0}}_{(1)}-\sum_{\mathbf{R}'}\boldsymbol{\delta}\mathbf{u}(\mathbf{R}')\underbrace{\sum_{\mathbf{R}}\nabla\Phi\big|_{\boldsymbol{\delta}\mathbf{u},\boldsymbol{\delta}\mathbf{u}'=0}}_{(2)} \end{aligned} \tag{5.48}$$

Focusing on (1) and (2) they represent the force of all the other atoms on the one fixed by the first summation. But since we said that the site of the lattice are the equilibrium position for the atoms, this means that the sum of all the forces on an atom, fixed in its lattice site, is zero. For this reason the second term is zero and thus we can rewrite eq. (5.47) as follows

$$U(\mathbf{r}_1,...,\mathbf{r}_N)=U_0+\frac{1}{2}\sum_{\mathbf{R},\mathbf{R}'}\sum_{\mu,\nu}\boldsymbol{\delta}\mathbf{u}_\mu(\mathbf{R})D_{\mu,nu}(\mathbf{R}-\mathbf{R}')\boldsymbol{\delta}\mathbf{u}_\nu(\mathbf{R}') \tag{5.49}$$

where we use the equal symbol thinking that the higher order contributions in the Taylor expansion can be neglected since they become smaller and smaller at higher orders; and where we introduce U_0 representing the potential energy of the system without any deviation from the equilibrium, and

$$D_{\mu,\nu} = \frac{1}{2}\delta_{\mathbf{R},\mathbf{R}'} \sum_{\mathbf{R}''} \left[\frac{\partial^2}{\partial r_\mu \partial r_\nu} \Phi(\mathbf{R} - \mathbf{R}'') - \frac{\partial^2}{\partial r_\mu \partial r_\nu} \Phi(\mathbf{R} - \mathbf{R}') \right]. \tag{5.50}$$

Using this, one can write the generic hamiltonian of the system as

$$H_{ph} = \sum_{\mathbf{R}} \frac{M}{2} \left(\frac{d\boldsymbol{\delta}\mathbf{u}(\mathbf{R})}{dt} \right)^2 + U_0 + \frac{1}{2} \sum_{\mathbf{R},\mathbf{R}'} \sum_{\mu,\nu} \boldsymbol{\delta}\mathbf{u}_\mu(\mathbf{R}) D_{\mu,\nu}(\mathbf{R} - \mathbf{R}') \boldsymbol{\delta}\mathbf{u}_\nu(\mathbf{R}') \tag{5.51}$$

One than can proceed by introducing the conjugate momentum to $\boldsymbol{\delta}\mathbf{u}$ that we will call $\boldsymbol{\delta}\mathbf{p}$ and rewrite the previous equation as

$$H_{ph} = \sum_{\mathbf{R}} \frac{\boldsymbol{\delta}\mathbf{p}^2(\mathbf{R})}{2M} + \frac{1}{2} \sum_{\mathbf{R},\mathbf{R}'} \boldsymbol{\delta}\mathbf{u}(\mathbf{R}) \cdot D(\mathbf{R} - \mathbf{R}') \boldsymbol{\delta}\mathbf{u}(\mathbf{R}') \tag{5.52}$$

where we rewrite the harmonic potential term in matrix form D. What we have done since this moment is done with a classical approach. To quantized this hamiltonian one can do in a very straightforward way by introducing the normal mode expansion of the displacement. This can be done by thinking at the general solution of the equation of motion, that can be written starting from hamiltonian (5.52)

$$M \frac{d^2}{dt^2} \boldsymbol{\delta}\mathbf{u}(\mathbf{R}) = \sum_{\mathbf{R}} D(\mathbf{R} - \mathbf{R}') \boldsymbol{\delta}\mathbf{u}(\mathbf{R}'). \tag{5.53}$$

The general solution can be written as a combination of plane waves that, using the periodic boundary condition, takes the form

$$\boldsymbol{\delta}\mathbf{u}_n = \sum_{\mathbf{k},m} C_{k,m} \varepsilon_m e^{i\mathbf{k}\cdot\mathbf{R_n} - i\omega_{\mathbf{k},m} t} \tag{5.54}$$

where one imposing the periodic boundary condition has that the summation over the k point is finite and is equal to the number of atoms in the system. By calling

$$Q_{k,m}(t) = C_{k,m} \varepsilon_m e^{-i\omega_{\mathbf{k},m} t} \sqrt{N} \tag{5.55}$$

one obtain the expansion in normal modes for the displacement

$$\boldsymbol{\delta}\mathbf{u}_n(t) = \frac{1}{\sqrt{N}} \sum_{\mathbf{k},m} Q_{k,m}(t) e^{i\mathbf{k}\cdot\mathbf{R_n}}. \tag{5.56}$$

Using this expression in (5.52) one obtain an equation equal in form to that of a set of decoupled harmonic oscillators

$$H_{ph} = \sum_{\mathbf{k},m} \frac{M}{2} \left(\left| \dot{Q}_{k,m} \right|^2 + \omega_m^2 \left| Q_{k,m} \right|^2 \right) \tag{5.57}$$

where $\dot{Q}$ stands for Q time derivative, and this can be easily quantized as a quantum harmonic oscillators introducing a pair of bosonic operators, the creation and annihilation bosonic operators $a, a^\dagger$, which satisfy the commutation relation $[a_{i,m}, a^\dagger_{j,n}] = \delta_{i,j}\delta_{m,n}$, leading to

$$\hat{H}_{ph} = \sum_{\mathbf{k},m} \hbar\omega_m \left(a^\dagger_{\mathbf{k},m} a_{\mathbf{k},m} + \frac{1}{2} \right) \tag{5.58}$$

where m is the mode of the oscillations.

5.5.2 Phononic hamiltonian for tBLG

In the last section we introduce the general procedure to obtain the quantized phononic hamiltonian. In this section we will apply what seen to the specific case of the tBLG. We start by introducing the general form of the hamiltonian for the atoms in the tBLG system, having in mind the considerations done for the generic case of the previos section, so we write as shown in [40]

$$H_{ph} = T + U_E + U_B \tag{5.59}$$

where

$$T = \sum_{l=1}^{2} \sum_{\mathbf{R}} \frac{M}{2} \dot{\mathbf{r}}^{(l)}_{\mathbf{R}} \tag{5.60}$$

is the kinetic contribution of the atoms,

$$U_E = \sum_{l=1}^{2} \sum_{\mathbf{R}} \frac{1}{2} \left\{ (\lambda + \mu) \left(u^{(l)}_{xx} + u^{(l)}_{yy} \right)^2 + \mu \left[\left(u^{(l)}_{xx} - u^{(l)}_{yy} \right)^2 + 4 (u^{(l)}_{xy})^2 \right] \right\} \tag{5.61}$$

is the elastic energy of strained, where $\lambda \simeq 3.25 eV\Omega/\text{Å}^2$ and $\mu \simeq 9.57 eV\Omega/\text{Å}^2$ (Ω is the area of the tBLG 1^{st} Moiré BZ) are the Lamé factors for graphene [41,42], and $u^{(l)}_{ij} = (\partial_i u^{(l)}_j + \partial_j u^{(l)}_i)/2$ is the strain tensor; and U_B has the form

$$U_B = \sum_{j=1}^{3} \sum_{\mathbf{R}} 2V_0 \cos \left[\mathbf{b}^M_j \cdot \mathbf{R} + \mathbf{b}_j \cdot (\mathbf{r}^{(2)}_{\mathbf{R}} - \mathbf{r}^{(1)}_{\mathbf{R}}) \right] \tag{5.62}$$

and is the inter-layer binding energy, where V_0 is the strength of the potential, $\mathbf{b}_j^M, j = 1, 2$ are the Moiré BZ primitive vectors and $\mathbf{b}_3^M = -\mathbf{b}_1^M - \mathbf{b}_2^M$, $\mathbf{b}_j, j = 1, 2$ are the unrotated graphene Moiré BZ primitive vectors and $\mathbf{b}_3 = -\mathbf{b}_1 - \mathbf{b}_2$; and we use the same notation for $\mathbf{r}$ as in (5.45). This hamiltonian can be separated in a symmetric and asymmetric part, i.e. splitted in $\mathbf{r}^{\pm} = \mathbf{r}^{(2)}_{\mathbf{R}} \pm \mathbf{r}^{(1)}_{\mathbf{R}}$. This can be seen by the usual technique of dealing with two body terms, and consist of splitting the position in a term for the position of the center of mass and a relative position term. Since the U_B terms depends directly only from $\mathbf{r}^-$ we will consider only the asymmetric part of the hamiltonian, since is the most relevant for the electron-phonon coupling. We are saying in other word that the major contribution to the electron-phonon coupling is coming from the relative displacement between the atoms [10]. Now we proceed with the splitting of $\mathbf{r}^-$ as done in (5.45) so introducing the displacement

$$\mathbf{r}^-(\mathbf{R}^-) = \mathbf{R}^- + \boldsymbol{\delta}\mathbf{u}^-_{\mathbf{R}^-}. \tag{5.63}$$

So we can write the general bosonic hamiltonian with the dependence on the displacement in the same form obtained in (5.52), this time for convenience expressing it in the momentum space, by writing the representation in the Moiré momentum space of the displacement

$$\boldsymbol{\delta}\mathbf{u}^-_{\mathbf{R}^-}(t) = \sum_{\mathbf{q}} \boldsymbol{\delta}\mathbf{u}^-_{\mathbf{q}}(t) e^{i\mathbf{q}\cdot\mathbf{R}^-} \tag{5.64}$$

and remembering that this time due to the change of coordinate (symmetric/asymmetric) the conjugate momentum is $\boldsymbol{\delta}\mathbf{p}^-_{\mathbf{q}} = \tilde{M}\boldsymbol{\delta}\mathbf{u}^-_{-\mathbf{q}}$, with $\tilde{M} = M/2$. Finally we can write the phononic hamiltonian for the tBLG as

$$H_{ph} = \sum_{\mathbf{q}\in MBZ} \left[\sum_{\mathbf{G}^M} \frac{1}{2\tilde{M}} \boldsymbol{\delta}\mathbf{p}^{-*}_{\mathbf{q}+\mathbf{G}} \boldsymbol{\delta}\mathbf{p}^-_{\mathbf{q}+\mathbf{G}} + \frac{1}{2} \sum_{\mathbf{G}^M, \mathbf{G}'^M} \boldsymbol{\delta}\mathbf{u}^{-*}_{\mathbf{q}+\mathbf{G}} D(\mathbf{G}, \mathbf{G}') \boldsymbol{\delta}\mathbf{u}^-_{\mathbf{q}+\mathbf{G}'} \right] \tag{5.65}$$

where * is the complex conjugate and $D_{\mathbf{q}}(\mathbf{G}, \mathbf{G}')$ is the matrix D of equation (5.52), in the momentum representation, coming from the asymmetric part of the harmonic approximation of the potential $U_B + U_E$ and has the form [10,40]

$$D_{\mathbf{q}}(\mathbf{G}, \mathbf{G}') = \frac{1}{2}\mathbf{K}_{\mathbf{q}+\mathbf{G}} \delta_{\mathbf{G}',\mathbf{G}} + \mathbf{V}_{\mathbf{G}-\mathbf{G}'} \tag{5.66}$$

where

$$\begin{aligned} \mathbf{K}_{\mathbf{q}} &= \begin{pmatrix} (\lambda+2\mu)q_x^2 + \mu q_y^2 & (\lambda+\mu) q_x q_y \\ (\lambda+\mu) q_x q_y & (\lambda+2\mu)q_y^2 + \mu q_x^2 \end{pmatrix} \\ \mathbf{K}_{\mathbf{G}} &= -2V_0 \sum_{j=1}^{3} h^j_{\mathbf{G}} \begin{pmatrix} b_{jx} b_{jx} & b_{jx} b_{jy} \\ b_{jy} b_{jx} & b_{jy} b_{jy} \end{pmatrix} \end{aligned} \tag{5.67}$$

where $b_{j\mu}$ is the μ component of the b_j as defined before, and $h^j_{\mathbf{G}}$ can be found solving

$$\cos\left[\mathbf{b}^M_j \cdot \mathbf{R} - b_j \cdot \mathbf{R}^-\right] = \sum_{\mathbf{G}} h^j_{\mathbf{G}} e^{i\mathbf{G}} \cdot \mathbf{R}. \tag{5.68}$$

By expanding then the displacement and its conjugate momentum in normal modes, and then by quantizing it, we obtain the general form of H_{ph} for the phononic hamiltonian

$$\hat{H}^r_{ph} = \sum_{m,\mathbf{q}\in MBZ} \hbar\omega_m \left(a^\dagger_{\mathbf{q},m} a_{\mathbf{q},m} + \frac{1}{2}\right) \tag{5.69}$$

where we write $\hat{H}$ to remember that after the quantization the hamiltonian is an operator. To find the frequencies for each modes, so the eigenfrequencies, one has to solve the equation of motion, that can be written as

$$\sum_{\mathbf{G}'} \hat{D}_{\mathbf{q}}(\mathbf{G},\mathbf{G}') Q_{\mathbf{q},m}(\mathbf{G}) = \tilde{M}\omega^2_{\mathbf{q},m} Q_{\mathbf{q},m}(\mathbf{G}) \tag{5.70}$$

5.5.3 Electron-electron interaction

Since the greatest contribution to the electron-phonon coupling is given by the relative displacement, by considering only this terms one can write the phonon hamiltonian, in the second quantization formalism, as

$$H_{ph} = \sum_{m,\mathbf{k}} \hbar\omega_{m,\mathbf{k}} \left(a^\dagger_{\mathbf{k},m} a_{\mathbf{k},m} + \frac{1}{2}\right) \tag{5.71}$$

where we remember $\mathbf{k} \in MBZ$, and the relative displacement in second quantization is

$$\boldsymbol{\delta u}_{\mathbf{R}} = \sum_{\mathbf{k},m} \vec{u}_{\mathbf{k},m} \sqrt{\frac{\hbar}{2\tilde{M}\omega_{m,\mathbf{k}}}} \left(a^\dagger_{\mathbf{k},m} + a_{-\mathbf{k},m}\right) e^{i\mathbf{k}\cdot\mathbf{R}} \tag{5.72}$$

Since the system under studying is the tBLG we can express directly $V(\mathbf{r})$ as

$$V(\mathbf{r}) = \sum_{\mathbf{R}} V_0\left(\mathbf{r} - \mathbf{R}\right) = \sum_{\mathbf{R}^{(1)}} V_0\left(\mathbf{r} - \mathbf{R}^{(1)}\right) + \sum_{\mathbf{R}^{(2)}} V_0\left(\mathbf{r} - \mathbf{R}^{(2)}\right) \tag{5.73}$$

but since if we center our system of reference on one layer, say the one labeled with 1, we can express $\mathbf{R}^{(2)}$ as function $\mathbf{R}^{(1)}$ by $\mathbf{R}^{(2)} = \mathbf{R}^{(1)} - \boldsymbol{\tau}^{(2)} + \mathbf{d}$. Now

we notice that the relative displacement influences the inter plane distance so we have $\mathbf{d}' = \mathbf{d} + \boldsymbol{\delta}\mathbf{u}$. so we can rewrite eq. 5.73 as

$$\begin{aligned} V(\mathbf{r}) &= \sum_{\mathbf{R}} \left[V_0 \left(\mathbf{r} - \mathbf{R} \right) + V_0 \left(\mathbf{r} - \mathbf{R} + \boldsymbol{\tau}^{(\mathbf{2})} - \mathbf{d}' \right) \right] = \\ &= \sum_{\mathbf{R}} \left[V_0 \left(\mathbf{r} - \mathbf{R} \right) + V_0 \left(\mathbf{r} - \mathbf{R} + \boldsymbol{\tau}^{(\mathbf{2})} + \mathbf{d} - \boldsymbol{\delta}\mathbf{u}_{\mathbf{R}} \right) \right] = \\ &\Big\downarrow \; V_0\left(\mathbf{r}-\mathbf{R}+\boldsymbol{\tau}^{(\mathbf{2})}+\mathbf{d}-\boldsymbol{\delta}\mathbf{u}_{\mathbf{R}}\right) \simeq V_0\left(\mathbf{r}-\mathbf{R}+\boldsymbol{\tau}^{(\mathbf{2})}+\mathbf{d}\right) - \boldsymbol{\delta}\mathbf{u}_{\mathbf{R}} \cdot \nabla V_0 + h.o. \\ &\simeq \sum_{\mathbf{R}} \left[V_0 \left(\mathbf{r} - \mathbf{R}^{(\mathbf{1})} \right) + V_0 \left(\mathbf{r} - \mathbf{R}^{(\mathbf{1})} + \boldsymbol{\tau}^{(\mathbf{2})} + \mathbf{d} \right) - \boldsymbol{\delta}\mathbf{u}_{\mathbf{R}} \cdot \nabla V_0 \right] = \\ &\simeq \sum_{\mathbf{R}^{(1)}} \left[V_0 \left(\mathbf{r} - \mathbf{R}^{(\mathbf{1})} \right) + \sum_{\mathbf{R}^{(2)}} V_0 \left(\mathbf{r} - \mathbf{R}^{(\mathbf{2})} \right) - \boldsymbol{\delta}\mathbf{u}_{\mathbf{R}} \cdot \nabla V_0 \right] \end{aligned} \tag{5.74}$$

The term which give the coupling between phonons and the electrons is the last term of the previous equation, since the first part is the unperturbed potential considered in the tight-binding approach. Using the second quantization expression of the relative displacement (5.72) we obtain the electron-phonon coupling, remembering the general dependence of the fermionic operators on the indeces $\eta = \pm 1$ for the valley, $\xi = \pm 1$ for the Moiré valley and $s = \pm 1$ for the spin, as

$$H^{e-p}_{\eta,\xi,s,\eta',\xi',s'}(\mathbf{k}) = -i \sum_{\mathbf{q},m} g_{m,\mathbf{q},\mathbf{k}} c^{\dagger}_{\mathbf{k}+\mathbf{q},\eta,\xi,s} \left(a^{\dagger}_{\mathbf{q},m} + a_{-\mathbf{q},m} \right) c_{\mathbf{k},\eta',\xi',s'} \tag{5.75}$$

5.5.4 BCS hamiltonian

To simplify the problem we can assume that the two contributions coming from the different modes are equal, so we can redefine the factor $g_{\mathbf{q},\mathbf{k}}$ incorporating the factor two in it. In the spirit of the BCS approach we introduce the BCS hamiltonian in the form of

$$H_{BCS} = \sum_{I,I'} \int d\mathbf{r} \left[\varepsilon c^{\dagger}_{I} c_{I'} - i g c^{\dagger}_{I} \left(a^{\dagger} + a \right) c_{I'} \right] \tag{5.76}$$

where the indices I, I' refer to all the possible quantum numbers $I = (\eta, \xi, s)$. Expressing the partition function in a path integral form, using the coherent states for bosons and fermions one has

$$\mathcal{Z} = \int D\left[\phi, \phi^*\right] \int D\left[\psi, \psi^*\right] e^{-S_{el}[\psi,\psi^*] - S_{ph}[\phi,\phi^*] - S_{BCS}[\psi,\psi^*,\phi,\phi^*]} \tag{5.77}$$

where ϕ are complex numbers associated to bosons and ψ are Grassmann variables associated to fermions. The free actions for bosons is in a gaussian form therefore we can integrate over the complex fields, obtaining an effective interactions among the fermions

$$H_{int} = \sum_{\mathbf{k},\mathbf{k}',\mathbf{q}} \sum_{\eta,\eta'} \sum_{\xi,\xi'} \sum_{s,s'} - g_{\mathbf{k},\mathbf{k}',\mathbf{q}} c^{\dagger}_{\mathbf{k}'+\mathbf{q},\eta,\xi,s} c^{\dagger}_{-\mathbf{k}',\eta',\xi',s'} c_{\mathbf{k}+\mathbf{q},\eta',\xi',s'} c_{-\mathbf{k},\eta,\xi,s} \quad (5.78)$$

where we suppose that this is an attractive interaction. Putting this term in the action and writing it in momentum space, we have

$$S^{eff}_{BCS} = \sum_{\mathbf{k},\mathbf{k}',\mathbf{q}} \sum_{\eta,\eta'} \sum_{\xi,\xi'} \sum_{s,s'} \Big[(-i\omega_n + \varepsilon_{\mathbf{k}})\, \psi^{\dagger}_{\mathbf{k},\eta,\xi,s} \psi_{\mathbf{k},\eta',\xi',s'} + \\ - g_{\mathbf{k},\mathbf{k}',\mathbf{q}} \psi^{\dagger}_{\mathbf{k}'+\mathbf{q},\eta,\xi,s} \psi^{\dagger}_{-\mathbf{k}',\eta',\xi',s'} \psi_{\mathbf{k}+\mathbf{q},\eta',\xi',s'} \psi_{-\mathbf{k},\eta,\xi,s} \Big] \quad (5.79)$$

5.5.5 Comment on the interaction

In the BCS hamiltonian (5.79), we had simply assume an attractive interaction among fermions mediated by phonons. This cannot be done in principle, because of the large number of couplings, so that some coupling channels could be attractive while others could be repulsive. What we are going to show is that the main component is an effective attractive interaction, and that only one pairing channel can be considered because it is dominant with respect to the others. A generic state of coupled fermions can be written as

$$|\psi_{I,I'}\rangle = \sum_{l\in\mathbb{Z},\mathbf{k}} A_{l,\mathbf{k}} c^{\dagger}_{\mathbf{k},\eta,\xi,s} c^{\dagger}_{-\mathbf{k},\eta',\xi',s'} |0\rangle \quad (5.80)$$

where $I = \eta, \xi, s$ is the set of quantum indices. The possible states, considering for example just the valley index, can be an inter-valley or an intra-valley pairing, i.e.

$$\begin{aligned} &|\psi_{(+,\xi,s),(+,\xi,s)}\rangle\,, |\psi_{(-,\xi,s),(-,\xi,s)}\rangle \text{ Intra-valley} \\ &|\psi_{(+,\xi,s),(-,\xi,s)}\rangle \text{ Inter-valley} \end{aligned} \quad (5.81)$$

To evaluate if the interaction mediated by the phonon with this state is attractive or repulsive one have to evaluate

$$\begin{aligned} E_{+,+} &= \langle\psi_{(+,\xi,s),(+,\xi,s)}|\, H_{int}\, |\psi_{(+,\xi,s),(+,\xi,s)}\rangle \\ E_{-,-} &= \langle\psi_{(-,\xi,s),(-,\xi,s)}|\, H_{int}\, |\psi_{(-,\xi,s),(-,\xi,s)}\rangle \\ E_{+,-} &= \langle\psi_{(+,\xi,s),(-,\xi,s)}|\, H_{int}\, |\psi_{(+,\xi,s),(-,\xi,s)}\rangle\,. \end{aligned} \quad (5.82)$$

We refer to the result of B. Liau, Z. Wang and B.A. Bernevig [10], who calculated this expectation values and see that the pairing that gives an attractive interaction is the inter-valley pairing. One has in general to study also the pairing using the other two indices, ξ and s. However since in general a time-reversal invariant interaction is more robust than a violating time-reversal one in the presence of disorder [43], one can fix the relation between the two remaining indices imposing the time-reversal invariant relation. Since under time-reversal symmetry $\mathbf{K} \to \mathbf{K}'$, $\mathbf{K}^M \to \mathbf{K}'^M$ and $s \to -s$, for the property of the Dirac hamiltonian, we will have

$$|\psi_{(\eta,\xi,s),(-\eta,-\xi,-s)}\rangle \tag{5.83}$$

as the strongest channel bringing attractive interaction between fermions.

5.5.6 Gap equation and critical temperature

Using this assumption for the pairing we can rewrite eq. (5.79) as follows

$$S^{eff}_{BCS} = \sum_{\mathbf{k},\mathbf{k}',\mathbf{q}} \sum_{\eta,\xi,s} \Big[(-i\omega_n + \varepsilon_{\mathbf{k}})\, \psi^\dagger_{\mathbf{k},\eta,\xi,s} \psi_{\mathbf{k},\eta,\xi,s} + \\ - g_{\mathbf{k},\mathbf{k}',\mathbf{q}} \psi^\dagger_{\mathbf{k}'+\mathbf{q},\eta,\xi,s} \psi^\dagger_{-\mathbf{k}',-\eta,-\xi,-s} \psi_{\mathbf{k}+\mathbf{q},-\eta,-\xi,-s} \psi_{-\mathbf{k},\eta,\xi,s} \Big] \tag{5.84}$$

In addition as a further approximation we will consider the strength of the coupling as constant. To decouple the interaction term one performs an Hubbard-Stratonovich transformation, introducing the field Δ

$$\mathcal{Z} = A \int D\left[\Delta, \bar{\Delta}\right] \int D\left[\psi, \psi^*\right] e^{-S^{eff}_{BCS}[\psi,\psi^*,\Delta,\bar{\Delta}]} \tag{5.85}$$

with

$$S^{eff}_{BCS}[\psi,\psi^*,\Delta,\bar{\Delta}] = \sum_{\mathbf{k},\mathbf{k}',\mathbf{q}} \sum_{\eta,\xi,s} \Big[(i\omega_n + \varepsilon_{\mathbf{k}})\, \psi^\dagger_{\mathbf{k},\eta,\xi,s} \psi_{\mathbf{k},\eta,\xi,s} - \frac{|\Delta_{\eta,\xi,s}(\mathbf{q})|^2}{g} + \\ + \bar{\Delta}_{\eta,\xi,s}(\mathbf{q}) \psi_{\mathbf{k},-\eta,-\xi,-s} \psi_{\mathbf{k},\eta,\xi,s} + \Delta_{\eta,\xi,s}(\mathbf{q}) \psi_{\mathbf{k},\eta,\xi,s} \psi_{\mathbf{k},-\eta,-\xi,-s} \Big] \tag{5.86}$$

Since we are interested in the low energy limit , at the mean field level, we can consider only the term $\mathbf{q} = (\vec{q}, \omega_l) = (0, 0)$ getting

$$S^{eff}_{BCS}[\psi, \psi^*, \Delta, \bar{\Delta}] \simeq \sum_{\mathbf{k},\mathbf{k}'} \sum_{\eta,\xi,s} \Bigg[(i\omega_n + \varepsilon_{\mathbf{k}})\, \psi^\dagger_{\mathbf{k},\eta,\xi,s} \psi_{\mathbf{k},\eta,\xi,s} - \frac{|\Delta_{\eta,\xi,s}|^2}{g} + \\ + \bar{\Delta}_{\eta,\xi,s} \psi_{\mathbf{k},-\eta,-\xi,-s} \psi_{\mathbf{k},\eta,\xi,s} + \Delta_{\eta,\xi,s} \psi_{\mathbf{k},\eta,\xi,s} \psi_{\mathbf{k},-\eta,-\xi,-s} \Bigg] \tag{5.87}$$

By using this approach one think of Δ as a physical field described as

$$\bar{\Delta}_{\eta,\xi,s} = \left\langle \psi^\dagger_{k,\eta,\xi,s} \psi^\dagger_{-k,-\eta,-\xi,-s} \right\rangle \tag{5.88}$$

where its value is different from 0 below the critical temperature, where the superconducting properties appears, and so where the Cooper pairs are present. By using this assumption for Δ one is treating the problem with a mean field calculation, in fact we are attributing a physical interpretation to the field introduced mathematically using the H-S transformation, as shown below

$$\begin{aligned} &\sum_{\mathbf{q},\mathbf{k},\mathbf{k}'} \psi^\dagger_{\mathbf{k}'+\mathbf{q}} \psi^\dagger_{-\mathbf{k}'} \psi_{\mathbf{k}+\mathbf{q}} \psi_{-\mathbf{k}} \overset{q=(0,0)}{\longrightarrow} \sum_{\mathbf{k}} \psi_{\mathbf{k}} \psi_{-\mathbf{k}} \sum_{\mathbf{k}'} \psi^\dagger_{\mathbf{k}'} \psi^\dagger_{-\mathbf{k}'} = \\ &\Big\downarrow \underbrace{a\bar{\Delta}}_{\text{Mean Field}} + \underbrace{\left(\textstyle\sum_{\mathbf{k}} \psi^\dagger_{\mathbf{k}} \psi^\dagger_{-\mathbf{k}} - a\bar{\Delta}\right)}_{\text{Small Fluctuations}} \\ &= \left[a\bar{\Delta} - \left(\sum_{\mathbf{k}} \psi^\dagger_{\mathbf{k}} \psi^\dagger_{-\mathbf{k}} - a\bar{\Delta} \right) \right] \left[a\Delta - \left(\sum_{\mathbf{k}'} \psi'_{\mathbf{k}} \psi_{-\mathbf{k}'} - a\Delta \right) \right] = \\ &= a^2 |\Delta|^2 + a\Delta \psi^\dagger \psi^\dagger + a\bar{\Delta} \psi\psi + \text{small fluctuations} \end{aligned} \tag{5.89}$$

Introducing the Nambu spinor $\Psi = (\psi_I, \bar{\psi}_{-I})^T$ we can write eq. (5.87)

$$= \sum_{\eta,\xi,s} \sum_{\mathbf{k}} \left[\frac{|\Delta_{\eta,\xi,s}|^2}{g} + \bar{\Psi} \mathcal{G}^{-1} \Psi \right] \tag{5.90}$$

with

$$\mathcal{G}^{-1} = \begin{pmatrix} i\omega_n + \varepsilon_{\mathbf{k}} & \Delta_{\eta,\xi,s} \\ \bar{\Delta}_{\eta,\xi,s} & i\omega_n - \varepsilon_{\mathbf{k}} \end{pmatrix} \tag{5.91}$$

From this, using the gaussian integral in the Grassmann variables, supposing that the interaction is equal for the interchange of the quantum numbers, one obtains

$$S^{eff}_{BCS}[\Delta, \bar{\Delta}] = 8 \left\{ \sum_{\mathbf{k}} \frac{|\Delta|^2}{g} - \ln\left[\det\left(\mathcal{G}^{-1} \right) \right] \right\} \tag{5.92}$$

and by minimizing the functional, if we suppose that $\bar{\Delta}$ is independent from $\mathbf{k}$ (since we are supposing that the interacting potential is independent from it), one finds the gap equation as

$$\begin{aligned} \frac{\partial S^{eff}_{BCS}}{\partial \Delta} &= 0 \\ \beta V \frac{\bar{\Delta}}{g} = \frac{\partial}{\partial \bar{\Delta}} Tr\left[\ln\left(\mathcal{G}^{-1}\right)\right] &= Tr\mathcal{G}_{(2,1)} \\ \frac{\bar{\Delta}}{g} &= -\frac{1}{\beta V}\sum_{\mathbf{k}} \frac{\bar{\Delta}}{\omega_n^2 + E^2_{BdG}} \end{aligned} \tag{5.93}$$

where we have defined $E_{BdG}(\vec{k}) = \varepsilon^2_{\mathbf{k}} + |\Delta|^2$. We can simplify the last equation and integrating in the Matsubara frequencies we have

$$\frac{1}{g} = \frac{1}{V}\sum_{\vec{k}} \left[\frac{tgh\left(\frac{\beta E_{BdG}(\vec{k})}{2}\right)}{2E_{BdG}(\vec{k})}\right] \tag{5.94}$$

Now looking at the density of states and band structure at the first magic angle, i.e. $\theta = 1.05°$, and at figure 5.6 (second picture from the top), we can notice that since the band is extremely flat and squashed on the Fermi level, we can approximate it with a small constant value. Is important to notice that below the T_c this means that since the unperturbed energy gap is $\simeq 0$ all the excitation spectrum E_{BdG} is dominated by the phonon induced excitation. Since our aim is to find an analytical expression for the critical temperature, we can proceed by noticing that T_c is defined by the transition of the order parameter Δ: Δ, the mean number of Cooper pairs, is different from zero only in the region below T_c, so as $T \to T_c$, $\Delta \to 0$. With this consideration we rewrite eq. (5.94) as follows

$$\frac{1}{g} = \frac{1}{V}\sum_{\vec{k}} \frac{tgh\left(\frac{\sqrt{\varepsilon^2_{\mathbf{k}}+|\Delta|^2}}{2k_BT_c}\right)}{2\sqrt{\varepsilon^2_{\mathbf{k}}+|\Delta|^2}} \xrightarrow{\Delta\to 0} \frac{1}{g} = \frac{1}{V}\sum_{\vec{k}} \frac{tgh\left(\frac{\varepsilon_{\mathbf{k}}}{2k_BT_c}\right)}{2\varepsilon_{\mathbf{k}}} \tag{5.95}$$

and by switching to the integral form to take the thermodynamic limit we have

$$\frac{1}{g} = \int \frac{d\mathbf{k}}{4\pi^2} \frac{tgh\left(\frac{\varepsilon_{\mathbf{k}}}{2k_BT_c}\right)}{2\varepsilon_{\mathbf{k}}} \tag{5.96}$$

now introducing the density of energy states defined as

$$\nu(\varepsilon) := \int_{\mathbb{R}^2} \frac{d\mathbf{k}}{4\pi^2} \delta(\varepsilon - E(\mathbf{k})) \tag{5.97}$$

we can write

$$\frac{1}{g} = \int d\varepsilon \nu(\varepsilon) \frac{tgh\left(\frac{\varepsilon}{2k_B T_c}\right)}{2\varepsilon} \tag{5.98}$$

now since we are only interested in the integral over the lowest band we set an energy cutoff to the integral: we know from experimental evidence, and as shown in our numerical calculation reported in figure 5.6, that the band is really flat so we could think to an energy interval $[-\delta, \delta]$ where δ represents the energy bandwidth. We write, approximating the density of states as a constant value inside this interval,

$$\frac{1}{g} = \nu_0 \int_0^{\delta} d\varepsilon \frac{tgh\left(\frac{\varepsilon}{2k_B T_c}\right)}{\varepsilon} \tag{5.99}$$

The main contribution to the integral comes from large energies for which the hyperbolic tangent ~ 1, and solving in terms of T_c one gets

$$T_c \simeq \frac{\delta}{2k_B} e^{-\frac{1}{g\nu_0}} \simeq 1.37K \tag{5.100}$$

where we used some real values taken from Ref. [10], $g \simeq 1\text{meV}$, $\nu_0 \gtrsim 1\text{meV}^{-1}$, and taking as band width $\delta \simeq 0.64\text{meV}$, obtained from our calculations. This result is in a good agreement with the experimental result reported in Ref. [9] and very close to the result obtained in [10], $T_c \simeq 0.9K$, where the authors just used the McMillan formula [14, 15]. The discrepancy, therefore, might come from the fact that the authors of [10] claim to go beyond the mean field approximation, taking into account also the screening effect. However our result shows that the mean field level is sufficient to provide a fairly good estimate for the critical temperature in this system.

Conclusions

In this work we reviewed the general approach useful to describe graphene, deriving the tight-binding description and its low energy limit. We showed how this model can be generalized to a system made of two layers of graphene, focusing in particular to the case of two layers disposed in a Bernal stacking (AB configuration). Then we studied the twisted bilayer graphene, i.e. a system of two graphene layers stacked in AB configuration, shifted by a small vector $\mathbf{d}$ and twisted with a relative angle θ. The system is particularly interesting because its properties can be modified upon varying the parameter θ, exhibiting a transition from an highly conducting state to an insulator. This behavior is related to the commensurability of the structure obtained by twisting the layers. For small twist angles the layers are in a commensurate state and this results in the appearance of a periodic pattern, the Moiré lattice. Indeed, one can verify that the physical properties of the twisted bilayer graphene are linked to the Moiré lattice constant and to the superposition between the atoms of the two layers. Studying the band structure and analyzing the density of states, that shows the presence of a Van Hove singularity in correspondence of the Fermi energy, one observes, for some specific values of θ, the appearance of flat bands.

After rederiving the tight-binding model for the tBLG, making explicit the dependence on the tunable parameter, we calculated the band structure numerically. We analyzed how the truncation in the Hamiltonian to a finite number of Moiré Brillouin zones influences the estimation of the energies. We then analyzed how the Fermi velocity, computed numerically, depends on the values of the angle finding those at which the velocity almost vanishes, the so-called magic angles. The value of the first magic angle obtained numerically is in perfect agreement with the analytical result obtained in the low energy limit.

In the last part of the thesis we focused on the first magic angle, consider-

ing the folded Hamiltonian valid in the low energy limit to study the form of the interaction. We rederived the phononic Hamiltonian, and use it to study the electron-electron interaction mediated by phonons. We showed how this interaction is particularly strong due to the presence of different coupling channels. We studied how the strength depends on different couplings. After verifying that this interaction is effectively an attraction, like in a BCS hamiltonian, by means of a path integral approach we derived the gap equation and obtained an estimate for the critical superconducting temperature, finding a good agreement with the experimental result [9].

Bibliography

[1] K.S. Novoselov, A.K. Geim, S.V. Morozov, S.V. Dubonos, Y. Zhang, D. Jiang, *Room-temperature electric field effect and carrier-type inversion in graphene films*, Nature manuscript 2004-02-15117, (2004)

[2] M. I. Katsnelson, K. S. Novoselov, A. K. Geim, *Chiral tunnelling and the Klein paradox in graphene*, Nature Physics volume 2, pages620625, (2006)

[3] Y. Zhang, Y. Tan, H. L. Stormer, P. Kim ,*Experimental observation of the quantum Hall effect and Berry's phase in graphene*, Nature volume 438, pages201204, (2005)

[4] A. H. Castro Neto, F. Guinea, N. M. R. Peres, K. S. Novoselov, *The electronic properties of graphene*, Rev. Mod. Phys. 81, 109 (2009), and A. K. Geim, https://link.aps.org/doi/10.1103/RevModPhys.81.109.

[5] R. Bistritzer and A. H. MacDonald, *Moiré bands in twisted double-layer graphene*, Proc. Natl. Acad. Sci. U.S.A. 108, 12233 (2011), https://doi.org/10.1073/pnas.1108174108.

[6] L. Balents, *General continuum model for twisted bilayer graphene and arbitrary smooth deformations*, SciPost Phys. 7, 048 (2019),doi: 10.21468/SciPostPhys.7.4.048.

[7] E. Suárez Morell, J. D. Correa, P. Vargas, M. Pacheco, and Z. Barticevic, *Flat bands in slightly twisted bilayer graphene: Tight-binding calculations*, Phys. Rev. B 82, 121407(R) (2010), https://doi.org/10.1103/PhysRevB.82.121407.

[8] Matthew Yankowitz, Shaowen Chen, Hryhoriy Polshyn, K. Watanabe, T. Taniguchi, David Graf, Andrea F. Young, Cory R. Dean, *Tuning superconductivity in twisted bilayer graphene*, Science (2019): Vol. 363, Issue 6431, pp. 1059-1064, doi: 10.1126/science.aav1910.

[9] Y. Cao, V. Fatemi, S. Fang, K. Watanabe, T. Taniguchi, E. Kaxiras, and P. Jarillo-Herrero, *Unconventional superconductivity in magic-angle graphene superlattices*, Nature (London) 556, 43 (2018).

[10] B. Lian, Z. Wang and B. A. Bernevig, *Twisted Bilayer Graphene: A Phonon-Driven Superconductor*, Phys. Rev. Lett. 122, 257002 (2019), doi:10.1103/PhysRevLett.122.257002.

[11] F.Wu, E. Hwang and S. Das Sarma, *Phonon-induced giant linear-in-t resistivity in magic angle twisted bilayer graphene: Ordinary strangeness and exotic superconductivity*, Phys. Rev. B 99, 165112 (2019), doi:10.1103/PhysRevB.99.165112.

[12] G. W. Semenoff, *Condensed-Matter Simulation of a Three-Dimensional Anomaly*, Phys. Rev. Lett. 53, 2449 (1984).

[13] S. Reich, J. Maultzsch, C. Thomsen, and P. Ordejon, *Tight-binding description of graphene*, Phys. Rev. B 66, 035412 (2002).

[14] W. L. McMillan, *Transition temperature of strong-coupled superconductors*, Phys. Rev. 167, 331 (1968).

[15] P. B. Allen and R. C. Dynes, *Transition temperature of strong-coupled superconductors reanalyzed*, Phys. Rev. B 12, 905 (1975).

[16] Alexander I. Cocemasov, Denis L. Nika, Alexander A. Balandin, *Phonons in twisted bilayer graphene*, Phys. Rev. B 88, 035428 (2013)

[17] L. D. Landau, L. P. Pitaevskii, A. M. Kosevich, E. M. Lifshitz, *Theory of elasticity*, (2012)

[18] A. V. Rozhkov, A. O. Sboychakov, A. I. Rakhmanov, F. Nori, *Electronic properties of graphene-based bilayer systems*, Physics Reports, 648:1104, (2016)

[19] Mei Zhang, *Handbook of Graphene, Volume 3: Graphene-like 2D Materials*, Publisher: Wiley-Scrivener, (2019)

[20] J. M. B. Lopes dos Santos, N. M. R. Peres, A. H. C. Neto, *Continuum model of the twisted graphene bilayer*, Phys. Rev. B, 86(15):155449, (2012)

[21] I. Brihuega, P. Mallet, H. Gonzlez-Herrero, G. Trambly de Laissardire, M. M. Ugeda, L. Magaud, J.M. Gmez-Rodrguez, F. Yndurin, J.-Y. Veuillen, *Unravelling the intrinsic and robust nature of van Hove singularities in twisted bilayer graphene*, Phys. Rev. Lett., 109(19):196802, (2012)

[22] S. Reich, J. Maultzsch, C. Thomsen, *Tight-binding description of graphene*, Phys. Rev. B, 66(3):035412, (2002)

[23] A. V. Rozhkov, A. O. Sboychakov, A. I. Rakhmanov, F. Nori, *Electronic properties of graphene-based bilayer systems*, Physics Reports, 648:1104, (2016)

[24] C. Bena and G. Montambaux, *Remarks on the tight-binding model of graphene*, New J. Phys., 11 (9):095003, (2009)

[25] G. Li, A. Luican, J. M. B. L. dos Santos, A. H. C. Neto, A. Reina, J. Kong, and E. Y. Andrei, *Observation of van Hove singularities in twisted graphene layers*, Nature Physics, 6(2):109113, (2010)

[26] J. Gonzalez, *Kohn-Luttinger Superconductivity in graphen*, Phys. Rev. B, 78(20):205431, (2008)

[27] D. Weckbecker, S. Shallcross, M. Fleischmann, N. Ray, S. Sharma, and O. Pankratov, *Low-energy theory for the graphene twist bilayer*, Phys. Rev. B, 93(3):035452, (2016)

[28] G. T. de Laissardiere, D. Mayou, and L. Magaud, *Numerical studies of confined state in rotated bilayer of graphene*, Phys. Rev., 86(12):125413, 2012.

[29] A. K. Geim and A. H. MacDonald, *Graphene: exploring carbon flatland*, Physics Today 60, 8, 35; https://doi.org/10.1063/1.2774096, (2007)

[30] M. I. Katsnelson, *Graphene: carbon in two dimensions*, Cambridge University Press, (2012)

[31] A. K. Geim. *Graphene: status and prospects*, Science, 324(5934):15301534, (2009)

[32] A. O. Sboychakov, A. Rakhmanov, A. V. Rozhkov, F. Nori, *Electronic spectrum of twisted bilayer graphene*, Physical Review B 92(7), doi: 10.1103/PhysRevB.92.075402, (2014)

[33] S. Carr, S. Fang, Z. Zhu, E. Kaxiras, *Exact continuum model for low-energy electronic states of twisted bilayer graphene*, Phys. Rev. Research 1, 013001, (2019)

[34] D. Wong, Y. Wang, J. Jung, S. Pezzini, A. M. DaSilva, H. Tsai, H. S. Jung, R. Khajeh, Y. Kim, J. Lee, S. Kahn, S. Tollabimazraehno, H. Rasool, K. Watanabe, T. Taniguchi, A. Zettl, S. Adam, A. H. MacDonald, M. F. Crommie, *Local spectroscopy of moir-induced electronic structure in gate-tunable twisted bilayer graphene*, Phys. Rev. B 92, 155409, (2015)

[35] S. Carr, D. Massatt, S. Fang, P. Cazeaux, M. Luskin, E. Kaxiras, *Twistronics: Manipulating the electronic properties of two-dimensional layered structures through their twist angle*, Phys. Rev. B 95, 075420, (2017)

[36] A. O. Sboychakov, A. L. Rakhmanov, A. V. Rozhkov, and Franco Nori, *Electronic spectrum of twisted bilayer graphene*, Phys. Rev. B 92, 075402, (2015)

[37] M. Koshino, N. F.Q. Yuan, T. Koretsune, M. Ochi, K. Kuroki, L. Fu, *Maximally Localized Wannier Orbitals and the Extended Hubbard Model for Twisted Bilayer Graphene*, Phys. Rev. X 8, 031087, (2018)

[38] N. Nagaosa, *Quantum field theory in condensed matter physics*, Publisher:

[39] G. Catarina, B. Amorim, E. V. Castro, J. M. Viana Parente Lopes, N. M. R. Peres, *Twisted bilayer graphene: low-energy physics, electronic and optical properties*, arXiv:1908.01556, (2019)

[40] M. Koshino, N. N. T. Nam, *Effective continuum model for relaxed twisted bilayer graphene and moir electron-phonon interaction*, Phys. Rev. B 101, 195425, (2020)

[41] K. V. Zakharchenko, M. I. Katsnelson, and A. Fasolino, *Finite Temperature Lattice Properties of Graphene Beyond the Quasiharmonic Approximation*, Phys. Rev. Lett. 102, 046808, (2009)

[42] J. Jung, A. M. DaSilva, A. H. MacDonald, and S. Adam, *Origin of band gaps in graphene on hexagonal boron nitride*, Nat. Commun. 6, 6308, (2015)

[43] P.W. Anderson, *Theory of dirty superconductors*, Journal of Physics and Chemistry of Solids 11, 26-30, (1959)